

AN EXPERIMENTAL INVESTIGATION
OF
HYPERSONIC STAGNATION TEMPERATURE
PROBES

Thesis by
Richard D. Wood

In Partial Fulfillment of the Requirements
For the Degree of
Aeronautical Engineer

California Institute of Technology

Pasadena, California

1959

ACKNOWLEDGMENTS

The research conducted during this program was carried out under the supervision of Professor Lester Lees and Dr. James Kendall, Jr. of the Jet Propulsion Laboratory. The author is also deeply appreciative of the wholehearted support he received from the Jet Propulsion Laboratory and particularly to Mr. Harris M. Schurmeier, Mr. Ralph Beal, and Mr. Robert Martin. Special thanks are due to Mr. C. A. Bartsch and Mr. Howard McDonald of the Aeronautical Machine Shop for the long hours and infinite patience that were required to fabricate the array of probes tested. To Mr. David Douglas, my associate at the Jet Propulsion Laboratory who was of invaluable assistance in conducting the program, a sincere expression of gratitude is extended. My thanks are also due to the staff of the Hypersonic Wind Tunnel for their assistance and advice during the many long hours of testing.

ABSTRACT

An experimental investigation of single-shielded hypersonic stagnation temperature probes was conducted in the GALCIT Leg No. 1 hypersonic wind tunnel and in the Jet Propulsion Laboratory 12-inch supersonic wind tunnel.

By the combined use of both shield and base heating, a probe recovery factor of $r = 1.0$ was obtained over a range of Reynolds numbers at $M_\infty = 5.75$. By using the experimental data and simple heat balance equations, the probe losses, for the conditions investigated, were found to be in the proportion:

shield conduction loss - 15

base conduction loss - 3

thermocouple conduction loss - 1

thermocouple radiation loss - $3/100$

The typical decrease in probe recovery factor observed for decreasing Reynolds number appears to be related to a decrease in the base temperature and not to the wire conduction loss as commonly assumed.

An optimum probe vent to entrance area ratio of $A_v/A_e \approx 1/2$ was found and is shown to be a function of the number of vent holes used in the shield.

No single calibration parameter was found that could relate the experimental recovery factors under all conditions.

TABLE OF CONTENTS

PART		PAGE
	Acknowledgments	
	Abstract	
	Table of Contents	
	List of Tables	
	List of Figures	
	List of Symbols	
I.	Introduction and Statement of Problem	1
II.	Facilities and Equipment	3
	A. Wind Tunnels	3
	B. Instrumentation	4
III.	Probe Description	6
	A. Design Criteria	6
	B. Construction	8
IV.	Test Procedure and Data Reduction	9
V.	Experimental Results and Analysis	11
	A. Base Heated Probe	11
	1. Analysis of Correlation Parameters	12
	B. Base and Shield Heated Probe	17
	1. Probe Loss Ratios	19
	C. Effect of Shield Vent Area	23
	1. Vent Area Variation	24
	2. Variation in Number of Shield Ventholes	25
	D. Ramp Probe	26
	E. Miscellaneous Probes	27

VI.	Summary and Conclusions	29
	References	31
	Appendix - A Thermocouple Conductive Heat Transfer	34
	Appendix - B Thermocouple Radiation Heat Transfer	39
	Appendix - C Base Conductive Heat Transfer	43
	Appendix - D Shield Conductive Heat Transfer	46
	Appendix - E Fabrication Technique	51

Tables

Figures

LIST OF TABLES

TABLE

- I Properties of Probe Materials
- II Physical Properties and Parameters of Base and Shield Heated Probe

LIST OF FIGURES

FIGURE

- 1 Thermocouple Circuit Diagram
- 2 Probe Heater Circuit Diagram
- 3 Schlieren Photographs of Base Heated Stagnation Temperature Probe
- 4 Thermal Conductivity of Probe Materials
- 5 Base and Shield Heated Stagnation Temperature Probe
- 6 Recovery Factor Versus Free Stream Reynolds Number at Two Stagnation Temperatures
- 7 Recovery Factor Versus Base Power
- 8 Recovery Factor Versus Thermocouple Convective Heat Transfer Coefficient For Two Stagnation Temperatures
- 9 Recovery Factor Versus Factor $(Nu_w K_g / K_w)$
- 10 Recovery Factor Versus Factor $(\rho_w / T_o)^{3/4}$
- 11 Thermocouple Conduction Heat Transfer Versus Free Stream Reynolds Number at $M = 5.75$
- 12 Probe Mass and Energy Flow Rate Versus Free Stream Reynolds Number at $M = 5.75$
- 13 Recovery Factors Versus Base and Shield Power at $T_o = 235^\circ F$
- 14 Recovery Factors Versus Base and Shield Power at $T_o = 310^\circ F$
- 15 Recovery Factor Versus Free Stream Reynolds Number for Base and Shield Probe at $M = 5.75$
- 16 Loss Ratios Versus Free Stream Reynolds Number for Base and Shield Heated Probe
- 17 Probe Loss Ratio Versus Total Power Supplied For Base and Shield Heated Probe, $P_b = 0.326$ Watts

FIGURE

- 18 Probe Loss Ratio Versus Total Power Supplied For Base and Shield Heated Probe, $P_b = 0.274$ Watts
- 19 Recovery Factor Versus Vent to Entrance Area Ratio at $M = 5.75$
- 20 Recovery Factor Versus Thermocouple Convective Heat Transfer Coefficient for Several Vent to Entrance Area Ratios at $M = 5.75$
- 21 Thermocouple Conduction Heat Transfer Versus Vent to Entrance Area Ratio at $M = 5.75$
- 22 Recovery Factor Versus Vent to Entrance Area Ratio at $M = 2.81$
- 23 Recovery Factor Versus Thermocouple Convective Heat Transfer Coefficient for Several Vent to Entrance Area Ratios at $M = 2.81$
- 24 Thermocouple Conduction Heat Transfer Versus Vent to Entrance Area Ratio at $M = 2.81$
- 25 Effect of Number of Vent Holes on Recovery Factor
- 26 Effect of Heated Base on Optimum Vent Hole Size and Number
- 27 Base Heated Ramp Probe
- 28 Recovery Factor Versus Angle of Attack For Ramp Probe
- 29 Tunnel Wall Temperature Boundary Layer Survey at $M = 5.75$
- 30 Tunnel Wall Temperature Boundary Layer Survey For Three Reynolds Numbers
- 31 Boundary Layer and High (L/D) Probe
- 32 Recovery Factors For Several Typical Probes

SYMBOLS

a	local speed of sound
A	cross-section area
c	constant
C_D	vent hole orifice discharge coefficient
C_V	specific heat at constant volume
C_P	specific heat at constant pressure
D	diameter
E	energy flow rate, Btu/sec
g	gravity constant = 32.2 ft/sec ²
K	thermal conductivity, Btu/sec in °R
L	length
L/D	length over diameter ratio of exposed single thermocouple wire
M	Mach number
h	convective heat transfer coefficient, Btu/sec in ² °R
Nu	Nusselt number
P	pressure
Pr	Prandtl number
q	heat transfer rate, Btu/sec
q_{ST}	total shield heat transfer rate, Btu/sec
R	gas constant or radiation parameter
Re	Reynolds number
(Re)*	Reynolds number based on stagnation conditions
r_x	recovery factor = $(T_x - T)/(T_o - T)$
r_e	equilibrium recovery factor for $r_1 = r_b$
S	surface area
T	local free stream temperature, °R

T ₀	stagnation temperature, °R
u	velocity
w	mass flow, lbs/sec
x	distance
a	$\left(\frac{1 - r_{s_1}}{s_1} \right)$
β	thermal boundary layer thickness
γ	ratio of specific heats = 1.4
ε	emissivity
ε _{w-s}	emissive interchange factor
μ	viscosity of air
φ	angle of attack
ρ	density
∇	Stefan-Boltzmann constant = 3.337×10^{-15} Btu/sec in ² (°R) ⁴

SUBSCRIPTS

a _t	adiabatic tube parameter
b	conditions at base of probe
e	condition at probe entrance
g	property of gas
i	indicated value
o	stagnation condition
p	internal probe shield parameter
s _i	inside shield surface parameter
s _o	outside shield surface parameter
t	supporting tube
T	total
v	property of shield vent

w values based on thermocouple wire

∞ free stream value

SUPERSCRIPTS

()' value based on conditions behind normal shock

I. INTRODUCTION AND STATEMENT OF PROBLEM

With the advent of hypersonic flight velocities, the accurate determination of the thermodynamic state of gases flowing at high velocities has become increasingly important. A particularly useful quantity is the stagnation state of the gas.

The measurement of the stagnation pressure presents no particular problem, except at very low Reynolds numbers and pressures, since a well designed pitot tube will usually measure the pressure with sufficient precision. Because of the well known difficulty of measuring the local temperature in a moving gas, one attempts, instead, to measure the local stagnation temperature (enthalpy). The local stagnation enthalpy is defined by the relation:

$$h_o = h + u^2/2$$

where (h) is the local enthalpy and (u) is the gas velocity. Stagnation enthalpy (h_o) is the value of enthalpy of the gas after it is brought to rest in a steady adiabatic compression and allowed to come to complete thermal equilibrium. For a calorically and thermally perfect gas the above relation becomes:

$$c_p T_o = c_p T + u^2/2$$

Together with the stagnation pressure and at least one other flow quantity (static pressure, density, etc.) the stagnation enthalpy completely determines the state of the gas.

Even at high Reynolds numbers the measurement of the stagnation temperature of a gas has proved to be not easily solved. In any real instrument the process of bringing the gas to rest always involves heat transfer and viscous stresses, so that the indicated temperature is

usually less than the actual stagnation temperature.

Numerous experiments (References 12, 32, 40) conducted with a large variety of stagnation temperature probes almost invariably result in an error or correction term that varies significantly with stagnation temperature, Mach number, and Reynolds number. Thus, a probe is of only qualitative value unless a complete calibration is available or a calibration parameter can be determined. The purpose of this investigation was to develop a probe which would not require such extensive calibration.

The principal heat transfer losses in the type of probe considered in this study are: thermocouple wire conduction and radiation, base conduction, and radial conduction through the enclosing shield. Even by using materials of the lowest possible thermal conductivity and optimum geometry, it was found that these losses are significant when compared to the forced convective heat transfer between the air sample and indicating thermocouple.

Since it appeared unlikely that a suitable calibration parameter could be developed that would allow correlation of the probe recovery factor to the desired degree under all conditions, a new approach to the problem was taken. By electrically heating the shield and base of the probe and determining their temperature by means of additional thermocouples, it was felt that the principal probe losses could be eliminated. Using this approach, it also appeared that the relative importance of the various probe losses could be determined.

Experiments using this type of probe were conducted in the GALCIT Hypersonic Wind Tunnel at $M = 5.75$ and in the JPL 12-inch Supersonic Wind Tunnel at $M = 2.81$.

II. FACILITIES AND EQUIPMENT

A. Wind Tunnels

The Leg No. 1 wind tunnel of the GALCIT hypersonic facility is of the continuous flow, closed return type, with a nominal fixed Mach number of 6.0 and a test section size of 5x5 inches. A complete description of the compressor plant and the associated instrumentation may be found in Reference 1. The reservoir pressure ranges between 10 and 90 psia with corresponding Reynolds numbers between 25,000 and 200,000 per inch. The maximum reservoir temperature is limited to about 325^oF and is automatically controlled. Starting at a point 22 inches downstream of the throat and extending for 4 inches the test section flow is axially uniform on the centerline, with the flow inclination in this region less than ± 0.1 degrees.

The Jet Propulsion Laboratory 12-inch supersonic wind tunnel was operated as a continuous, closed-circuit tunnel for the program. Any value of test-section Mach number between 1.27 and 4.04 may be set by means of jacks which control the curvature of the flexible-plate nozzle. For Mach numbers up to 2.20, the test section is 12 inches square; and for Mach numbers above this value it is 12 inches wide and 9 inches high. . During a given run, the air supply is maintained at a constant temperature, and normally at a dew point sufficiently low to insure that dew-point effects on the data are negligible. The reservoir pressure ranges between 32 and 320 cm Hg absolute and the corresponding Reynolds numbers are between 50,000 and 500,000 per inch. The test section Mach number variation is less than $\pm .02$ and the flow inclination in this region less than ± 0.1 degrees.

B. Instrumentation

The tunnel stagnation temperature and the individual temperatures of the probe being tested were measured by identical iron-constantan thermocouples. The circuit diagram is shown in Figure 1. A "null-reading" Leeds and Northrup slide wire potentiometer was employed to read the resultant e.m.f. in the thermocouple circuit. The "null" method can be read to about 0.0001 millivolts, or $1/300^{\circ}\text{F}$, for an iron-constantan thermocouple. Since no current flows in this system when it is balanced, the circuit resistance does not enter into the measurement. The reference junction was lacquered with glyptal and inserted in a plugged glass tube filled with silicone fluid. The tube was surrounded by ice in a thermos bottle. Each thermocouple was read individually and was not connected in any way to the tunnel heater control system or to each other.

Table 2-30 in Reference 6 gives the thermocouple temperature limits and uncertainty intervals for several common thermocouple materials. This table indicates, for example, that the temperature error for a standard iron and constantan thermocouple can vary by as much as $\pm 4^{\circ}\text{F}$ for a temperature range of 0 to 530°F and as much as $\pm 3/4$ percent for temperatures up to 1400°F . Therefore, for precision temperature measurement, the same material, off the same roll, should be used in any system of thermocouples and, if absolute readings are important, each thermocouple should be carefully calibrated. An excellent discussion of the above and related thermoelectric problems is given in References 6 and 31.

Several of the probes employed a resistance heater coil with a circuit diagram as shown in Figure 2. Because of the very small amount of power required and excessive power line fluctuations, it was found

necessary to insert a constant voltage transformer in the supply line. By using vacuum tube voltmeters to read the circuit voltage and current, it was possible to resolve the power supplied to within .01 watts.

The reservoir pressure in Leg No. 1 was measured with a Tate-Emery nitrogen balanced gage and controlled within ± 0.04 psi by a Minneapolis-Honeywell Brown circular-chart controller. Static and stagnation impact pressures were measured with a silicone fluid, vacuum-referenced manometer. With this instrument, pressures can be read to the closest 0.1 cm and estimated to 0.01 cm of silicone fluid.

III. PROBE DESCRIPTION

A. Design Criteria

Several previous investigations of stagnation temperature probes have shown that certain design features are desirable. Because of their small size and adaptability to precision measurement, thermocouples are usually used as the sensing element in a probe. Temperature probes used at supersonic speeds and elevated temperatures usually employ several shields around the sensing thermocouple. The shields are used to direct the flow, minimize radiation losses, maintain known flow conditions around the thermocouple, and minimize heat loss from the air sample being measured. E. Winkler of the Naval Ordnance Laboratory (Reference 40) has demonstrated that by the proper choice of materials and design, a single-shielded probe can be made to give a very high recovery factor. It is also apparent that a small probe is necessary for use in boundary layer and wake study surveys in hypersonic wind tunnels.

In the use of a single shielded probe, the problem consists of arranging the thermocouple junction within the shield so that it will receive the maximum amount of heat from the air sample but lose the minimum amount of energy by radiation to the shield and by conduction down the wires into the base.

In general, there are two possibilities as to the shape of the shield for use in supersonic flow. It can either be long and thin, with an attached bow shock wave, or it can be short and blunt, with a detached bow shock wave. Actually, the position of the normal shock wave directly in front of the probe entrance is determined to a large extent by the ratio of vent to entrance area of the shield since the vent area controls

the mass flow through the probe. Excess flow "spills" around the shield. This behavior is clearly shown in Figure 3. A long thin shield has the disadvantages of considerably more surface area and a thin sharp entrance edge. This type of shield will allow considerable heat loss through the shield and will provide length for internal boundary layer growth before the flow reaches the thermocouple junction. Graves and Quiel (Reference 11) found that this type of shield reduced the probe recovery factor, while E. Winkler (Reference 40) found the probe recovery factor to be quite insensitive to shield design.

In the case of a short blunt shield, the air sample undergoes a more rapid expansion to a low subsonic velocity and possible internal flow separation due to the inherent adverse pressure gradient. If the thickness of the internal boundary layer becomes of the same order as the internal shield radius, the effect of conduction through the shield will be felt by the junction. If flow separation occurs, the mixing of cold wall flow with the center core will reduce the temperature of the junction. On the other hand, advantages of the blunt shield are its insensitivity to flow angle-of-inclination and a shorter distance between the entrance of the probe and the thermocouple junction.

The present study was also concerned with very small boundary layer probes having small internal area. Regardless of the design of the shield it will probably not be possible to escape the effects of heat transfer through the shield, therefore it was felt a short, relatively blunt shield should be used. This assumption appears to be verified by the experimental data. The general type of probe tested is shown in Figure 5. It is discussed in detail in Section V.

B. Construction

It is apparent from the preceding discussion that the material, finish, and size of the shield, the base, and the thermocouple are parameters affecting the temperature recovery of the probe. Also, for hypersonic wind tunnel operation up to $M \approx 9.0$, stagnation temperature would reach 1200°F . Therefore the probe had to be constructed entirely from materials capable of continuous operation at these elevated temperatures.

The thermocouples used throughout the probe and supply section were 0.010- or 0.005-inch diameter iron-constantan wire with fiberglass insulation. Two materials were used for the shield. By employing special techniques, as discussed in Appendix E, it was possible to construct shields from a zirconia-base ceramic. This type of shield was particularly desirable because of its excellent thermal shock resistance and, as shown in Figure 4, very low thermal conductivity. The second material used was a 96 per cent silica glass (Vycor) made by Corning Glass Works. Vycor glass may be generally compared with fused quartz in properties and performance. Both of the materials used have very low thermal conductivities as compared with other materials such as cermets and metals.

Since a considerable degree of precision was required in the construction of the probes, special fabrication techniques were developed and these techniques are discussed in detail in Appendix E. Construction difficulties constituted the biggest single problem in the entire program.

IV. TEST PROCEDURE AND DATA REDUCTION

The probe to be tested was mounted in the wind tunnels in an adjustable support so that the probe could be leveled and placed on the centerline of the tunnel.

The tunnel stagnation temperature was determined in GALCIT Leg No. 1 wind tunnel by making horizontal surveys across the tunnel 1.25 inches ahead of the throat. A small rake consisting of three shielded thermocouples and two stagnation pressure probes was used. Surveys were taken across the tunnel and the readings were corrected for a time variation in tunnel temperature as indicated by a fixed thermocouple in the entrance piping ahead of the turbulence damping screens. The flow corrected in this manner is uniform to within 1 degree Fahrenheit across the nozzle. The variation in the pressure was negligible. The temperature measured in the entrance piping and indicated by a Brown circular-chart controller was from 10 to 15 degrees high at all times.

Surveys made by R. Covey of the temperature distribution perpendicular to the direction of flow in the settling chamber of the JPL 12-inch wind tunnel indicated a uniform temperature distribution. Therefore a single shielded probe was placed at the centerline of the chamber. The tunnel temperature was normally measured by a probe inserted into the flow from the side of the chamber was also read during the program. This instrument read from 1 to 7 degrees low at all times as compared to the probe mounted on the center line and depended on the length of time the tunnel had been running. A probe mounted on the side wall of a tunnel will almost invariably read low because of the conduction loss from the probe into the cold wall. During a particular run each thermo-

couple was read and converted to temperature reading in degrees Fahrenheit. The actual reading was rounded off to the nearest 0.1 degree. The particular temperature was then used in computing a "recovery factor" from:

$$r_x = \frac{T_x - T}{T_o - T}$$

where the tunnel stagnation temperature, (T_o), used was the average of the three values indicated by the reservoir rake. The free stream static temperature, (T), was computed from the above stagnation temperature and the calibrated Mach number.

V. EXPERIMENTAL RESULTS AND ANALYSIS

Previous theoretical analyses of probes of this type by E. Winkler of N.O.I. (Ref. 40) and M. Scadron and I. Washawsky of NACA (Ref. 32) indicate that a major probe loss is the conductive heat transfer along the thermocouple wires into the base of the probe.

A. Base Heated Probe

To investigate the wire conduction loss phenomenon a probe was built with a small nicrome wire heater in the base as shown in Figure 5. To measure the temperature of the base, a second thermocouple (T_b) was buried within the coiled heater.

For calibration purposes a probe "recovery factor" is defined as:

$$r_i = \frac{T_i - T}{T_o - T}$$

where T_i = indicated temperature

T_o = actual stagnation temperature

T = free stream static temperature

A recovery factor of $r_i = 1$ indicates complete adiabatic recovery of the kinetic energy of the air flow.

If the recovery factor of the base is defined as:

$$r_b = \frac{T_b - T}{T_o - T}$$

then the base temperature and the probe indicated temperature may be compared in convenient dimensionless form.

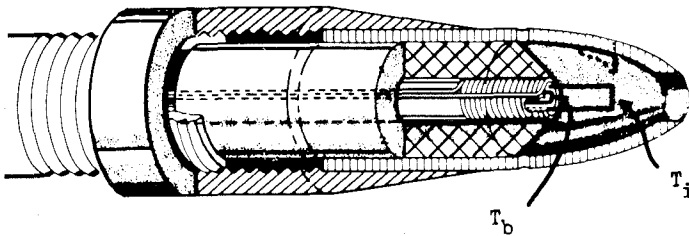
The variation of the probe and base recovery factors as a function of free stream Reynolds number for $M_{\infty} = 5.75$ and tunnel stagnation temperatures of 235 and 310°F is shown in Figure 6. The curves exhibit the typical decrease in recovery factor as the Reynolds number is decreased or the stagnation temperature is increased. The diameter of the

probe entrance (D_e) was used as the characteristic length in determining the free stream Reynolds number (Re).

If energy is supplied to the small base heater until the condition $T_i = T_b$, or $r_i = r_b$ is obtained, then the wire conduction loss is essentially eliminated. This conclusion is considered in detail in the following section. A typical plot of the variation of r_i and r_b as a function of base power is shown in Figure 7. Although the increase in the probe recovery factor is significant, other losses must be present since r_i and r_b are both less than one.

1. Analysis of Correlation Parameters

The approximation can be made that the heat transfer along the thermocouple wire may be characterized as the case of a uniform rod connected between identical heat sinks as shown below:



The forced convection heat transfer coefficient between the air sample and thermocouple may be determined from the relation:

$$h_w = \frac{K_w}{4D_w(L/D_w)^2} \left\{ \cosh^{-1} \frac{r_e - r_b}{r_e - r_i} \right\}^2$$

as developed in Appendix A. The radiation heat transfer from the wire is neglected and the condition $r_1 = r_b$ is called r_e . In the derivation of this equation, the recovery factor (r_e) or the temperature (T_e) is the air sample temperature and is independent of the temperature of the heat sinks. In the actual use of the base heater in the probe, it is impossible to decrease the temperature gradient along the thermocouple wires without decreasing the heat transfer rate between the air sample and the exposed end of the base; thus, the temperature of the air sample actually changes slightly. The recovery factor, (r_e) is then the air sample temperature in the absence of the wire and base conduction loss. Since the factor (r_e) enters the heat transfer coefficient equation in the form of a ratio, it is felt that the error is not significant in determining the order-of-magnitude numbers we are seeking, especially in view of the many other assumptions already made to obtain this equation. The heat transfer coefficient calculated on this basis is shown in Figure 8.

On the basis of an analysis by Scadron and Warshawsky, E. Winkler concluded that the probe recovery factor should be a function of a parameter:

$$r = f \left(N_{aw} \frac{K_g}{K_w} \right)$$

if the radiation error is small. The above parameter is actually a form of the Biot number often used in transient heat flow calculations and is the ratio of the surface heat transfer coefficient to the thermal resistance of the thermocouple wire when the diameter is used as the

significant length. Therefore:

$$P = f \left(\frac{h_w D_w}{K_w} \right)$$

Actually this parameter can be expressed in many forms such as:

$$Nu_w \frac{K_g}{K_w} = C Re_w^{1/2} Pr^{1/3} \frac{K_g}{K_w}$$

The relationship between the Nusselt number (Nu_w), the Reynolds number (Re_w), and the Prandtl numbers (Pr) was found by means of dimensional analysis (Reference 27), with the empirical coefficients being determined for the case of a circular cylinder in crossflow.

If the internal Reynolds number (Re_w), Prandtl number (Pr), and K_g and K_w are all expressed in terms of the stagnation temperature (T_0) and the constants are lumped together, Winkler found that:

$$\left(Nu_w \frac{K_g}{K_w} \right)^2 \approx f \left(\frac{P_w}{T_0^{3/4}} \right) = f \left(\frac{P_w}{T_0^{7/4}} \right)$$

where P_w and ρ_w are the internal static pressure and density at the thermocouple junction.

Plots of our experimental recovery factors versus ($Nu_w \frac{K_g}{K_w}$) and ($\rho_w/T_0^{3/4}$) are shown in Figures 9 and 10. The figures differ because the actual heat transfer coefficient as shown in Figure 8 was used in computing ($Nu_w \frac{K_g}{K_w}$) while the factor ($\rho_w/T_0^{3/4}$) was computed from the assumed normal shock recovery pressure, internal Mach number, and the actual tunnel stagnation temperature.

In neither case is any correlation evident for a change in stagnation temperature while holding the Mach number constant. In contrast, Winkler was able to obtain excellent correlation using either of the above para-

meters. The Winkler data differs in one respect, in that an increase in stagnation temperature was always accompanied by an increase in free stream Mach number which may help to explain the discrepancy between the respective results. In an initial study, an approximate copy of the Winkler probe was built, but the performance fell far short of the expected results even with the apparent advantage of a far lower stagnation temperature. This result, as well as the data obtained by Graves and Quiel (Reference 11) for a similar probe is shown in Figure 32.

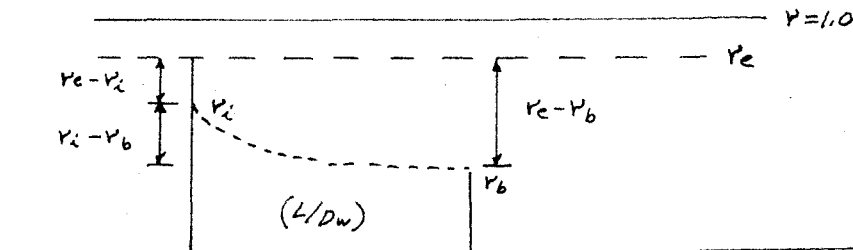
The parameter $(Nu \frac{K_g}{K_w})$ can also be written as

$$Nu_w \frac{K_g}{K_w} = \frac{1}{4 (L/D_w)^2} \left\{ \cosh^{-1} \frac{r_e - r_b}{r_e - r_i} \right\}^2$$

where the length over diameter ratio (L/D_w) of the thermocouple wire is a constant for a given probe. It is evident that the function will depend equally on the temperature of the probe base as well as the indicating thermocouple temperature and the air sample temperature.

If we sketch out a typical situation, it would appear as shown

below:



where the value (r_e) is the air sample temperature discussed previously. The wire and base conductive losses have been essentially eliminated in the determination of (r_e) or (T_e) , so the remaining difference $(1 - r_e)$ or $(T_o - T_e)$ must be the shield conduction and thermocouple wires radiation loss (see section V-B).

Now, the experimental data shown in Figure 6 indicates that the temperature difference ($r_1 - r_b$) remained nearly constant over the entire Reynolds number range tested. Since the wire heat transfer coefficient (h_w) and the function ($Nu_w K_g/K_w$) are determined by r_e as well as r_1 and r_b , and the variation of r_e with Reynolds number for the two stagnation temperatures tested is quite different, there is little reason to expect that any correlation of the experimental data with either of the parameters should exist in the present case.

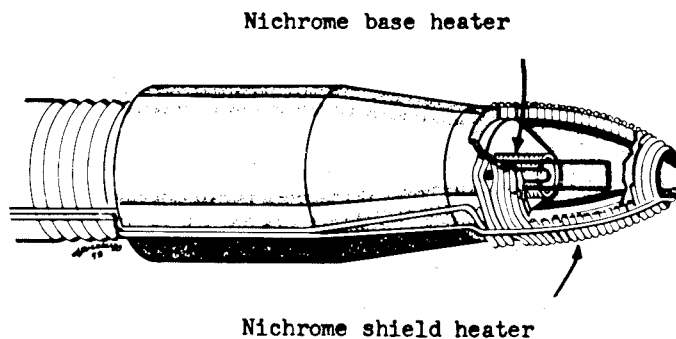
A second interesting point is brought out if we calculate the heat transfer rate along the thermocouple wires from:

$$q_w = \pi \sqrt{K_w h_w D_w^3} T_o \left(1 - \frac{T}{T_o}\right) \left\{ \tanh \sqrt{\frac{4 h_w}{K_w D_w} \left(\frac{L}{D_w}\right) D_w} \right\} (r_e - r_b)$$

The results, as shown in Figure 11, indicate that the heat transfer rate is almost constant over the range of the data. Therefore, use of the rather vague assumption of a relative increase in the wire conduction loss as compared to the convective heat transfer to explain the decrease in the recovery factor (r_1) of the probe does not seem to describe the actual physical phenomenon. For the data shown, the decrease in probe recovery factor (r_1) for decreasing Reynolds number is determined by the variation of the base recovery factor (r_b) and/or the shield conduction loss as indicated by (r_e).

B. Base and Shield Heated Probe

In an effort to determine and eliminate the remaining probe losses which were apparent from the base heated tests, a nichrome wire heater was coiled upon the outer surface of a second shield as shown below:



Additional thermocouples, as shown in Figure 5, were attached to the inside (T_{s_i}) and outside (T_{s_o}) of the shield and to the stainless steel support tube (T_t). A recovery factor for these temperatures is defined in the same manner as for the base temperature.

Typical variation of these five temperatures as a function of the base and shield energy supplied is shown in Figures 13 and 14. The data shown was obtained by application of heat to the base until an approximate matching point, $T_i = T_b$. Heat was then supplied to the shield while holding the power supplied to the base at a constant value. Examination of the data leads to the following conclusions:

1. In the unheated condition, the base and outside temperatures are the same.
2. Near-laminar temperature recovery is obtained on the surface of the stainless tube before heating.

3. A definite temperature gradient exists through the shield and the temperature difference remains constant regardless of the heat supplied to the probe.

A reduction in the base power is shown by the dashed lines in Figure 13. If the amount of heat supplied to the base and shield is adjusted until $T_i = T_b = T_{s_1}$, the wire conduction loss, base heat loss, radiation from the thermocouple wires, and conductive heat transfer through the shield are virtually eliminated. In the case shown, the thermocouples were matched with $r_i = .999$, $r_b = .999$, and $r_{s_1} = 1.004$, which corresponds to a temperature within one degree of the actual stagnation temperature.

Thus, the simultaneous heating of the shield and base would appear to allow the probe to obtain a recovery factor of 1.0 and to be maintained at this figure by the proper amount and ratio of energy supplied by the base and shield heaters.

The variation of indicated probe recovery factor (r_i) and base recovery factor (r_b) over the Reynolds number range in the unheated, base heated and shield heated conditions is compared with results of the base heated probe in Figure 15. The oblong symbols indicate the degree to which the condition $r_i = r_b = r_{s_1}$ was obtained by manual adjustment of the two-heater-power-supply Variacs. The decrease in the unheated recovery factors can probably be attributed to an increase in conduction losses through the shield due to the nichrome wire and cement around the outside surface. Also, in this case it was not possible to coat the shield with platinum or gold, so the radiation losses were increased slightly.

1. Probe Loss Ratios

By using the five experimental values obtained above, it was possible to obtain order-of-magnitude numbers of the various probe losses by means of simple heat balance equations derived in the Appendix.

a. Thermocouple Wire Conduction Loss

The thermocouple-wire conduction heat transfer was introduced in the preceding section in analyzing the results obtained with a base heated probe. The actual loss, in the form of a ratio (q_w/E), is shown in Figure 11 for the base heated probe and in Figure 16 for the base and shield heated probe.

The actual mass and energy flow rates were calculated from:

$$W = 0.003705 \left(\frac{P_0'}{P_0} \right) P_0 \left(\frac{A_w}{A_c} \right) A_e \frac{C_D}{\sqrt{T_0}} \quad \text{Lb/Sec}$$

and

$$E = 4.0 \times 10^{-5} W C_p T_0 \quad \text{Btu/Sec}$$

where C_D = vent orifice discharge coefficient.

Since the pressure ratio across the vent orifice (P/P_0') is always far below the critical value, a sonic throat exists in the vent passage. Experimental results of A. Weir (Reference 36) indicate an expression of:

$$C_D = 1 - 0.656 D_v$$

for the orifice discharge coefficient under sonic conditions.

For either probe, the loss ration (q_w/E) increases with a decrease in the free stream Reynolds number because of a decrease in the probe energy flow rate (E), while the actual loss (q_w) remains virtually constant.

b. Base Conduction Loss

If we consider the base heat transfer rate as a case of a long rod protruding from a heat source (Appendix C), a heat balance between the free stream air flow around the support tube and the tube itself can be written:

$$h_t = \frac{K_t D_t}{4(L_t)^2} \left\{ \ln \frac{r_b - r_{at}}{r_t - r_{at}} \right\}^2$$

where:

- h_t = film heat transfer coefficient between the tube and air-stream boundary layer.
- r_t = recovery factor of the tube at a distance L_t from base or heat source.
- r_{at} = adiabatic surface temperature recovery factor.
- r_b = base recovery factor

Since the boundary layer around the tube is probably laminar at the high Mach number tested, an adiabatic recovery factor $r_{at} = 0.85$ was assumed.

A heat transfer rate can then be found from:

$$q_b = q_c = \frac{\pi}{2} \sqrt{K_t h_t D_t^3} T_o \left(1 - \frac{T}{T_o}\right) (r_b - r_{at})$$

The loss ratio (q_b/E) is also shown in Figure 16. In general, the value of this ratio is approximately 3 times that of the wire conduction loss and shows the same general increase with decreasing Reynolds numbers as (q_w/E).

c. Thermocouple Radiation Loss

If the thermocouple radiation loss may be characterized as a case of diffuse reflection from the surfaces of two concentric cylinders heated by the flow of a non-radiating gas, the relation is given in Appendix B as:

$$q_r = \sigma \epsilon_{w-s} S_w T_o^4 (r_w^4 - r_{s_i}^4)$$

where:

$$\epsilon_{w-s} = \frac{1}{\frac{1}{\epsilon_w} + \frac{S_w}{S_{s_i}} \left(\frac{1}{\epsilon_{s_i}} - 1 \right)}$$

in which:

S_w and S_{s_i} are the surface areas of the wire and shield

ϵ_w and ϵ_{s_i} are the emissivities of the above surfaces

r_w and r_{s_i} are the recovery factors of these surfaces

is the Boltzman constant = 3.337×10^{-15} Btu/sec in² (°R)⁴

This heat transfer rate was calculated and expressed in loss ratio form in Figure 16. The value is a very small and roughly 3 parts in a hundred of the thermocouple conduction loss ratio.

d. Shield Conduction Loss

By setting up a local heat balance between the inner and the outer surfaces of the shield at the point where the surface recovery factors were measured and determining the local convective heat transfer coefficient of the inner surface, an estimate of the constant in the internal heat transfer - Reynolds number relationship:

$$(Nu)_{s_i} = C_{s_i} Pr^{1/3} (Re^*)_{s_i}^{3/4}$$

can be found (Reference 27). If this expression is applied over the whole axial length of the internal shield contour and the inside surface temperature is assumed to vary linearly from the value of T_0 at the entrance to the indicated value at a distance x_{s_i} , then the shield conduction heat transfer may be found from the relation:

$$Q_{ST} = \alpha \pi T_0 \left(1 - \frac{T}{T_0}\right) K_s \int_0^{x_c} (Nu)_x D_x dx$$

where:

$$\alpha = \frac{(1 - r_{s_i})_{local}}{x_{s_i}}$$

The value of (q_{ST}) was found by numerical integration using Simpson's rule and the relation:

$$D_x = 0.20 \sqrt{1 - 16x^2}$$

for the internal shield contour (The complete derivation is given in Appendix D). The loss ratio (q_{ST}) is shown in Figure 16. The value of q_{ST} is very high and, in fact, is about three times the sum of the other losses. Since the result could be expected to be correct to at least an

order of magnitude, there is a clear indication that the shield conduction loss must play an important role in affecting the indicated recovery factor of a small shielded probe. This result also seems to be borne out by the results obtained by heating the shield.

The combined probe losses are shown in Figure 16 as (q_T/E) .

e. Effect of Base and Shielding Heating on Probe Losses

If, for a particular flow condition, we assume that the convective heat transfer coefficients of the base (h_b) and internal shield surface (h_{s_1}) do not change as the result of heating the base or the shield, the variation in the various probes losses as a function of the heat energy supplied may be calculated. This calculation has been carried out for the experimental data in Figure 13 and the results are shown in Figures 17 and 18. Negative values of the loss ratios indicate that the direction of the normal heat transfer has been reversed. From Figure 18 it is evident that the losses must be reduced to a very small percentage of the internal heat flow value to obtain a recovery factor of $r_1 \approx 1.0$.

C. Effect of Shield Vent Area

The general principle underlying the use of a number of small vent holes in the shield is to provide a continuous replacement of the air sample being measured; otherwise, the various probe heat flux losses would continuously decrease the temperature of the sample until a low equilibrium value is reached. To insure the maximum forced convective heat transfer to the indicating thermocouple junction and internal probe surfaces, the largest possible vent area should be used since the mass or energy flow rate is proportional to this parameter. The upper limit of this area is at a point at which the internal boundary layer over the thermocouple junction decreases the recovery factor (r_1). The relationship between

the total vent area (A_v) and the internal shield area (A_p) at the thermocouple junction also determines the Mach number at this point. For example, in the case of the base and shielded heated probe, the area ratio, $A_p/A_o = 37.50$, gives an internal Mach number of $M_w = 0.0155$, or about 20 ft/sec for the conditions tested, if the internal-shield-boundary layer buildup is neglected.

1. Vent Area Variation

Since it is difficult to estimate the optimum area ratio to use in the design of a probe, a series of runs was made using the base heated probe in the JPL 12-inch supersonic wind tunnel and in GALCIT Leg No. 1. The variation in the vent area was accomplished by drilling oversize holes in the Vycor glass shield, plugging the holes with Adweld cement and progressively drilling out the cement. The number of vent holes was held constant at 4 and the results are shown in Figures 19 and 22. Values of the indicated recovery factor (r_i) and base recovery factor (r_b) are shown and also the condition when $r_i = r_b$. The data indicates an optimum value of about $A_v/A_e \approx 0.60$ at $M_\infty = 5.75$ and $A_v/A_e \approx 0.40$ at $M_\infty = 2.81$. A slight shift to a lower value of (A_v/A_e) is observed when the base and wire conduction losses are eliminated by making $r_i = r_b$. These data agree fairly well with those obtained by Goldstein and Scherrer (Reference 12) for $M = 1.5$ with a similar 4-vent hole probe, but disagree with the optimum value of $A_v/A_e = 0.20$ found by Winkler for a 2-vent hole probe at $M = 4.9$.

If we make use of the equations for the thermocouple conduction loss, previously discussed in part A, we may calculate the convective heat transfer coefficient (h_w) as a function of the vent area, or the mass flow within the probe. The results are shown in Figures 20 and 23.

In this case, the coefficient actually seems to correlate fairly well with the probe recovery factor except at values of A_v/A_e approaching 1.0, where internal boundary layer build-up on the thermocouple junction will tend to decrease the recovery factor. The Mach number at this point is ≈ 0.10 .

Since the value of h_w is related to the Winkler correlation parameter ($Nu_w K_g/K_w$) by the constant ratio (D_w/K_w) it is apparent that the data would correlate as well with the parameter. For a similar variation in vent hole area at $M_\infty = 4.9$ for a 2-vent-hole probe, Winkler's data did not correlate with the above parameter.

The actual thermocouple heat transfer rate was also determined and was plotted versus the area ratio A_v/A_e in Figures 21 and 24. As expected, the maximum conduction loss occurs at the point of maximum probe temperature recovery, but the value increases as the free stream Reynolds number decreases because of the decrease in base recovery temperature. The loss ratio (q_w/E) was also determined and did not change appreciably for the two Mach numbers and stagnation temperatures investigated. An interesting schlieren photograph of the flow distribution around the probe at the two extremes of area ratio, $(A_v/A_e) = 0$ and 1.0, is shown in Figure 3.

2. Variation in Number of Shield Vent Holes

At the conclusion of the above investigation it became apparent that the actual number of vent holes must enter into the determination of the optimum vent to entrance area ratio. Using the same base heated probe, the investigation was partially repeated for the same area ratio at $M_\infty = 2.81$, but with 1 and 2 vent holes instead of 4. The results are shown in Figures 25 and 26. In the case of the single-vent-hole probe, the

optimum area ratio decreased to about $A_v/A_e = .25$ and did not change for the 2 vent holes, although the maximum recovery factor decreased. In the case of the heated base, the recovery factor increased only slightly, but the optimum area ratio decreased to about $A_v/A_e = .15$ for the single vent hole and to $A_v/A_e = .30$ for the 2-vent hole shield. The advantage of a probe with several vent holes appears to be related to the more symmetrical flow distribution of the air sample, as indicated by the increased base recovery factor. The corresponding increase in the area ratio to obtain optimum conditions can probably be related to a decrease in the vent area orifice discharge coefficient for the very small holes required.

D. Ramp Probe

Previous data clearly indicate the desirability of maintaining a high level of pressure or density of the air sample around the thermocouple junction. In an effort to improve the stagnation pressure recovery of the base heated probe, a two-shock, external-compression-inlet type of shield was built as shown in Figure 27. Such a probe would have the added advantage of being able to obtain values in the boundary layer close to a wall and yet be relatively large. By changing the angle of attack of the probe in the tunnel, the results shown in Figure 28 were obtained. The pressure recovery data were obtained with a probe using the same shield but replacing the base heater and base thermocouple with a pressure load. Because of the viscous lip effects around the ramp and inlet (0.05 in^2), it was necessary to use an angle of attack of almost 10 degrees before the normal shock pressure ratio could be obtained. Actually, because of a malfunction in the tunnel reservoir pressure measuring device, these

data could be in error by as much as $\pm .01$ in the pressure ratio. Note that the maximum temperature and pressure recoveries occur at different angles of attack. The overall effect is to improve the recovery factor, as compared to the normal shock type of shield.

The probe was also used to make the first measurements of the thickness of the thermal boundary layer along the floor of the test section in the GALCIT Leg No. 1. These results are shown in Figures 29 and 30. One observes that the base recovery factor follows the relative change in stagnation temperature. Although the recovery factor is increased by the use of the base heater, almost the same relative profile is observed. The value of β is the thickness, in inches, of the thermal boundary layer. The profile at the low Reynolds number has the general shape of the adiabatic stagnation temperature distribution or $(\partial T/\partial y)_{y=0} = 0$.

E. Miscellaneous Probes

In the course of the investigation, a number of other probes were built. The performance of these probes, as shown in Figure 32, is compared with that of the base heated probe (#1) previously discussed.

1. Probe #2 is an exact copy of the base heated probe without the heater. Also, a change in the junction was made from a cylinder in cross-flow to a thin flat plate perpendicular to the flow. Performance of the probe was less satisfactory than for probe #1.
2. A probe (#3), of the general design of the base heated probe, was built with a base and shield of ceramic, except that the lengths of the shield and thermocouple wires were increased to allow a wire length over diameter ratio (L/D) of 100 (Figure 31). A thin coat of ceramic cement was baked on the exposed wire to strengthen the probe. The increase in L/D tended to

decrease the slope of the recovery factor, but the overall performance decreased.

3. An approximate copy of the N.O.L. probe (#4) developed by E. Winkler was built from sketches in her report. Performance of the probe was less than the two previously discussed.
4. A very small unheated boundary-layer-type probe (#5), as shown in Figure 32, was built. The performance of the probe is low, but seems to fall in line with the data obtained for the base heated probe in the unheated condition.
5. Data obtained by Winkler at N.O.L. and Graves and Quiel (Reference 11) in GALCIT Leg No. 1 are shown for comparison.

VI. SUMMARY AND CONCLUSIONS

The results of the experimental stagnation temperature probe investigation indicate the following:

1. The use of a heated base probe to eliminate wire conduction loss and base heat transfer increases the performance of a probe significantly, but the recovery factor will remain less than 1.0.
2. Correlation of the data for two different stagnation temperatures at a Mach number of 5.75 by use of the parameter $(Nu_w K_g / K_w)$ as suggested by E. Winkler was unsuccessful, the parameter does not appear to adequately describe the actual physical phenomenon with sufficient accuracy for general use.
3. The typical decrease in recovery factor observed as the Reynolds number is decreased appears to be related to a decrease in the base temperature and not to the wire conduction loss as commonly assumed.
4. The use of a combined base and shield heated probe allows a recovery factor of $r = 1.0$ to be obtained, since all of the significant probe losses can be eliminated.
5. By using experimental data obtained for the base and shield heated probe, probe losses in terms of a percent of the probe energy flow rate were determined. The losses increase with decreasing Reynolds number or increasing stagnation temperature. These losses are roughly in the following proportions:

Shield Conduction Loss - 15

Base Conduction Loss - 3

Thermocouple Conduction Loss - 1

Thermocouple Radiation Loss - 3/100

6. An optimum ratio of vent to entrance area was found to be $A_v/A_e \approx .50$ for a probe with 4 vent holes. The optimum vent to entrance area ratio was found to be a function of the number of vent holes used, with a larger number being more desirable.
7. The use of a probe with an inlet ramp allows measurements of the thermal boundary layer to be made close to the wall with a relatively large probe.

Construction of several very small, single heated probes capable of a constant recovery factor of $r \approx 1.0$, for use in the Jet Propulsion Laboratory new 21-inch hypersonic wind tunnel, is underway at the present time. A servo system will be used to automatically control the energy supplied by the heater.

REFERENCES

1. Baloga, Paul, E.; Nagamatsu, Henry, T.: Instrumentation of GALCIT Hypersonic Wind Tunnels, Hypersonic Wind Tunnel Memorandum No. 29 July, 1955.
2. Blackshear, P. L., Jr.: Sonic-Flow-Orifice Temperature Probe for High-Gas-Temperature Measurements, NACA TN 2167. September 1950.
3. Brown, A. I.; Marco, S. M.: Introduction to Heat Transfer, McGraw-Hill, 1951.
4. Catalog: Nichrome, Driver-Harris Company R-58, 1958.
5. Dahle, A.; Flock, E. F.: Shielded Thermocouples for Gas Turbines, Trans. ASME 71, 153 (1949)
6. Dean, Robert C.: Aerodynamic Measurements, Gas Turbine Laboratory, Massachusetts Institute of Technology, Eagle Enterprises, Boston, 1953.
7. Eber, G. R.: "Shielded Thermocouples", High Speed Aerodynamics and Jet Propulsion, Volume IX, Physical Measurements in Gas Dynamics and Combustion, Princeton University Press, 1954.
8. Eckert, E. R. G.: Intrudction to the Transfer of Heat and Mass, McGraw-Hill, New York, 1950.
9. Eckert, E. R. G.; Drake, Robert M., Jr.: Heat and Mass Transfer, McGraw-Hill, 1959.
10. Franz, A.: Pressure and Temperature Measurement in Supercharger Investigations, NACA TM No. 953, 1940.
11. Graves, J. C.; Quiel, N. R.: Impact Pressure and Total Temperature Interpretation at Hypersonic Mach Number, GALCIT Hypersonic Wind Tunnel, Memorandum No. 20, July, 1954.
12. Goldstein, D. L.; Scherrer, R.: Design and Calibration of a Total-Temperature Probe for Use at Supersonic Speeds, NACA TN 1585, May 1949.
13. Hottel, H. C.; Kalitinsky, A.: Temperature Measurements in High-Velocity Air Streams, J. Appl. Mech, March, 1945.
14. Howard, W. R.: Wind Tunnel Testing at The Jet Propulsion Laboratory, Jet Propulsion Laboratory Report No. 20-83, January, 1957.
15. Jakob, M.; Hawkins, G. D.: Heat Transfer and Insulation, Wiley, 1947.

16. Jakob, Max: Heat Transfer, Vol. 1, Wiley, 1949.
17. Jakob, Max: Heat Transfer, Vol. II, Wiley, 1957.
18. Johnson, Neil, R.; Wenstein, A. S.; Osterle, F.: The Influence of Gradient Temperature Fields On Thermocouple Measurements, AFRC-TR-57-231, September, 1957.
19. Johnson, H. A.; Rubesin, M. W.: Aerodynamic Heating and Convective Heat Transfer-Summary of Literature Survey, Trans ASME, July, 1949.
20. Keenan, J. H.; Kaye, J.: Gas Tables, Wiley, 1948
21. King, W. J.: Measurement of High Temperatures in High Velocity Gas Streams, ASME, Vol. 65, 1943.
22. Kreith, F.: Principals of Heat Transfer, International, 1958.
23. Kuethe, A. M.; Schetzer, J. D.: Foundations of Aerodynamics, Wiley, 1950.
24. Laufer, John; McClellan, R.: Measurements of Heat Transfer From Fine Wires In Supersonic Flows, Jet Propulsion Laboratory, Report No. 20-101, June, 1956.
25. Liepmann, H. W.; Roskko, A.: Elements of Gas-Dynamics, Wiley, 1957.
26. Lindsay, W. F.: Calibration of Three Temperature Probes And A Pressure Probe at High Speeds, NACA, April, 1942.
27. McAdams, William H.: Heat Transmission, McGraw-Hill, 1942.
28. Moffatt, E. M.: Errors in High Temperatures Probe for Gases, ASME 48-A-52, 1948.
29. Mullikin, H. F.: Temperature, Its Measurement and Control in Science And Industry, Reinhold, 1941.
30. Rietdyk, J. A.; Valstar, A.: On a Thermoeter With Recovery Factor $r > 1$, Applied Science Research, Section A, Vol. 7, 1958.
31. Roeser, Wm. F.: Thermoelectric Thermometry, J. Appl. Phys., June, 1940.
32. Scadron, M. D.; Warshawsky, I.: Experimental Determination of Time Constants and Nusselt Numbers for Base-Wire Thermocouples in High Velocity Air Streams and Analytic Approximation of Conduction and Radiation Errors, NACA TN 2599, January, 1952.
33. Shapiro, Archer, H.: The Dynamics and Thermodynamics of Compressible Fluid Flow, Volumes I and II, Ronald Press, 1953.

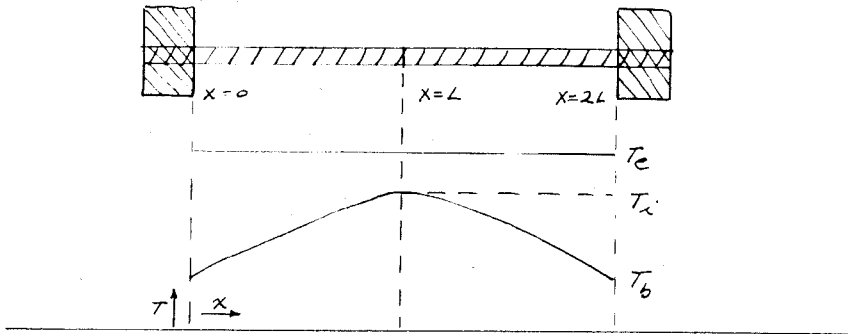
34. Spivak, H. M.: Experiments in the Turbulent Boundary Layer of a Supersonic Flow, North American Aviation Report CM-615, 1950.
35. Stolder, J. R.; Goodwin, G.; Craeger, M. O.; Heat Transfer to Bodies in a High-Speed Rarefied-Gas Stream, Trans. ASME, July, 1949.
36. Weir, A.; York, J. L.; Morrison, R. B.: Two-and Three-Dimensional Flow of Air Through Square-Edged Sonic Orifices, Trans. ASME, April, 1956.
37. Wimmer, W.: Stagnation Temperature Recordings, NACA-TM 967, 1941.
38. Winkler, E. M.: Design and Calibration of Stagnation Temperature Probes For Use at High Supersonic Speeds and Elevated Temperatures, J. Appl. Phys., February, 1954.
39. Winkler, E. M.: NOL Hypersonic Tunnel No. 4, Results IV, High Supply Temperature Measurements and Control, Navord Report 2574, 1952.
40. Winkler, E. M.: Stagnation Temperature Probes for Use at High Supersonic Speeds and Elevated Temperatures, Navord Report 3834, October, 1954.

APPENDIX A

THERMOCOUPLE CONDUCTIVE HEAT TRANSFER

A. General Equations

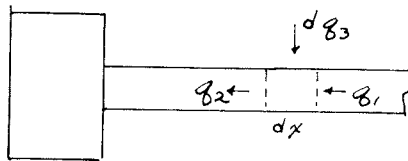
Consider the case of a uniform rod connected between two identical heat sinks as shown below (Reference 16):



If we neglect cross-sectional temperature differences as compared with the axial temperature distribution, we may use the elementary one-dimensional conduction heat transfer equation:

$$q = -K A \frac{dT}{dx} \quad (A-1.0)$$

Then, for an element of the rod between x and $x + dx$, and steady-state heat flow



$$q_2 = q_1 + dq_3$$

or
$$\frac{d^2T}{dx^2} = m^2 (T_c - T) \quad (A-1.1)$$

where

$$m^2 = \frac{hC}{KA}$$

in which

- K = thermal conductivity of the rod material
- A = rod cross-sectional area
- T = temperature of the rod
- T_e = environment temperature at the surface of the rod
- C = circumference of the rod
- h = surface or film heat transfer coefficient between the rod and the environment
- q = heat transfer per unit time

If we assume m is a constant, we have the standard form of an ordinary, second-order linear differential equation with constant coefficients. The general solution of this equation is:

$$(T_e - T) = c_1 e^{mx} + c_2 e^{-mx} \quad (A-1.3)$$

where C_1 and C_2 are constants of integration.

Applying the boundary conditions:

$$T = T_b \quad \text{or} \quad (T_e - T) = (T_e - T_b) \quad \text{at} \quad x=0 \quad \text{and} \quad x=2L$$

and a condition of no axial heat flow at $x = L$ or:

$$\frac{dT}{dx} = 0 \quad \text{at} \quad x=L$$

gives a solution:

$$(T_e - T) = \frac{(T_e - T_b)}{(1 + e^{m2L})} \left[e^{m(2L-x)} + e^{mx} \right] \quad (A-1.4)$$

We are interested in the temperature of the rod at $x = L$:

$$(T_c - T_x) = (T_c - T_b) \frac{2}{e^{-mL} + e^{mL}} = \frac{T_c - T_b}{\cosh(mL)} \quad (A-1.5)$$

Utilizing equation (A - 1.0) and the condition of symmetry around the center of the rod, we may calculate the total heat transfer from:

$$Q_T = 2 Q = hc \int_{x=0}^{x=2L} (T_c - T) dx$$

which has a solution of:

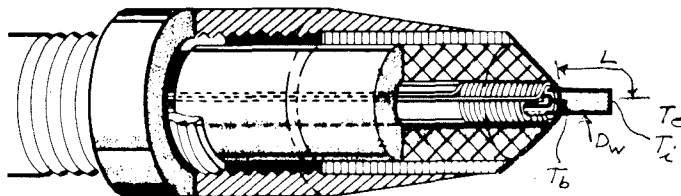
$$Q_T = 2 \sqrt{KhAC} \frac{e^{mL} - e^{-mL}}{e^{mL} + e^{-mL}} (T_c - T_b)$$

or

$$Q_T = 2 \sqrt{KhAC} \left[\tanh \sqrt{\frac{hc}{KA}} L \right] (T_c - T_b) \quad (A-1.6)$$

B. Specific Solution

An application of the general equations may be made in the following manner:



In the actual case, the rod is a thermocouple consisting of a loop of two dissimilar wires and the heat sink is the holder or base of the probe.

We define:

- L = exposed length of one wire
- D_w = diameter of wire
- T_i = indicated thermocouple junction temperature
- T_b = temperature of the base and of the thermocouple wires at junction with the base.
- T_e = thermocouple junction temperature in absence of wire conduction loss.

The thermocouple junction temperature is then related to the wire convective heat transfer coefficient by equation (A-1.5):

$$(T_e - T_i) = \frac{(T_e - T_b)}{\cosh\left(\sqrt{\frac{h_w c_w}{k_w A_w}} L\right)}$$

Solving for the wire heat transfer coefficient

$$h_w = \frac{k_w}{4 D_w (L/D_w)^2} \left\{ \cosh^{-1} \frac{r_e - r_b}{r_e - r_i} \right\}^2 \quad (A-1.7)$$

where T_e , T_b , and T_i are expressed in dimensionless recovery factor form,

$$r_K = \frac{T_K - T}{T_0 - T}$$

T_0 = Free stream stagnation temperature

T = Free stream static temperature

and D_w is the diameter of the thermocouple wire with (L/D_w) the ratio of the exposed length of a single wire to its diameter. The thermocouple wire thermal conductivity (K_w) is taken as the mean of the values of the

two dissimilar metals. In a similar manner, the total conductivity heat transfer is given by:

$$Q_w = \pi \sqrt{k_w h_w D_w^3} T_0 \left(1 - \frac{T}{T_0}\right) \left\{ \tanh \sqrt{\frac{4 h_w}{k_w D_w}} \left(\frac{L}{D_w}\right) D_w \right\} (T_c - T_b)$$

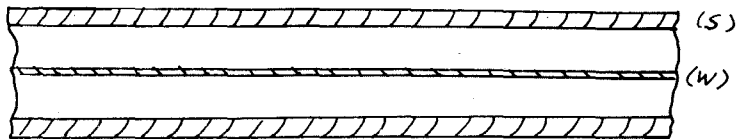
(A-1.8)

APPENDIX B

THERMOCOUPLE RADIATION HEAT TRANSFER

A. General Equations

Consider the case of two concentric cylinders heated by the flow of a nonradiating gas whose surfaces reflect diffusely (Reference 9).



If we define:

B_W = total (emitted plus reflected) radiative flux leaving cylinder (W) per unit time and surface area.

B_S = total radiative flux leaving the inside of cylinder (S) per unit time and surface area.

S_W = cylinder (W) surface area.

S_S = cylinder (S) surface area.

F_{a-b} = geometric shape factor (surface a views surface b)

e = emitted radiation flux per unit time and surface area

α = absorption coefficient

The total radiative flux from cylinder (W) is then $S_W B_W$ and from cylinder (S) the flux is $S_S B_S$. Now, only part of the flux from (S) actually impinges on (W) in the amount $F_{S-W} S_S B_S$.

Since the shape factors between the two surfaces are related by:

$$S_W F_{W-S} = S_S F_{S-W}$$

and (W) is completely surrounded by (S), therefore

$$F_{W-S} = 1 \quad \text{and} \quad F_{S-W} = \frac{S_W}{S_S}$$

Then the net radiative heat flow from (W) is the difference between the radiation arriving and leaving:

$$q_{sw} = S_w (B_w - B_s)$$

The total radiative flux from (W) consists of emitted and reflected radiation:

$$B_w = e_w + (1 - \alpha_w) B_s$$

In the case of cylinder (S), the total radiation leaving consists of emitted radiation, reflected radiation from (W), and reflected radiation from (S):

$$B_s = e_s + (1 - \alpha_s) F_{s-w} B_w + (1 - \alpha_s) (1 - F_{s-w}) B_s$$

Solving the previous three equations for q:

$$q = \frac{\alpha_s e_w - \alpha_w e_s}{\alpha_s + \frac{S_w}{S_s} (\alpha_w - \alpha_w \alpha_s)}$$

From the basic definition of the Stefan-Boltzman law,

$$e_B = \sigma T^4$$

and Kirchhoff's law,

$$e = \alpha e_B$$

or

$$\frac{e}{e_B} = \alpha = \epsilon$$

where e_B = total emitted black body radiation for the same temperature
as

σ = Stefan-Boltzman constant

ϵ = emissivity of surface of cylinder

Then we can write the radiation heat flux q as:

$$q_R = \epsilon_w S_w = \sigma \epsilon_{w-s} S_w (T_w^4 - T_s^4) \quad (B-1.0)$$

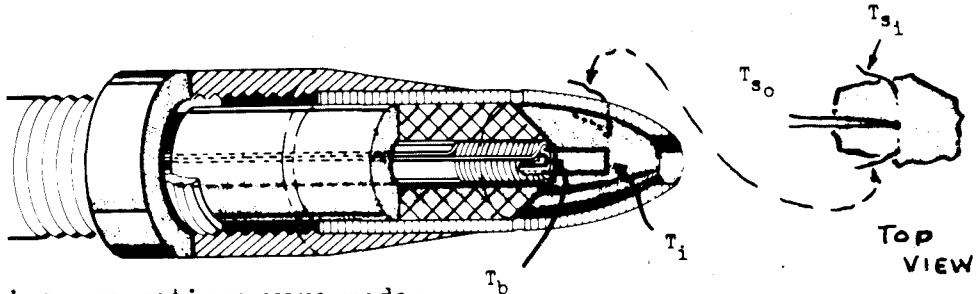
where

$$\epsilon_{w-s} = \frac{1}{\frac{1}{\epsilon_w} + \frac{S_w}{S_s} \left(\frac{1}{\epsilon_s} - 1 \right)} \quad (B-1.1)$$

q_R = net radiation flux from (W) per unit time

B. Specific Solution

In applying the general equations to the problem of radiation heat transfer from a shielded thermocouple wire as shown below:



the following assumptions were made:

1. Radiation heat transfer through the open end of the shield and the thermocouple wires is neglected.
2. Radiative interchange between the two dissimilar wires of the thermocouple is negligible.
3. Radiative interchange between the thermocouple wires and the shield with the base is neglected.
4. The entire exposed length of the thermocouple wire and the inside surface of the shield are assumed to be at a uniform temperature of T_i and T_{s_i} respectively.

If we express T_i and T_{s_i} in dimensionless recovery factor form,

$$r_K = \frac{T_K - T}{T_0 - T}$$

where: T_0 = Free stream stagnation temperature

T = Free stream static temperature

and make the further assumption that:

$$\frac{T_K - T}{T_0 - T} \approx \frac{T_K}{T_0}$$

we may write the expression for the radiation heat transfer between the thermocouple wires and the inside surface of the shield as:

$$Q_R = \epsilon_{w-s} S_w T_0^4 (T_i^4 - T_{s,i}^4) \quad (B-1.2)$$

where:

$$\epsilon_{w-s} = \frac{1}{\frac{1}{\epsilon_w} + \frac{S_w}{S_{s,i}} \left(\frac{1}{\epsilon_{s,i}} - 1 \right)} \quad (B-1.3)$$

in which:

S_w = exposed surface area of thermocouple
 $= 2\pi D_w^2 (L/D_w)$

$S_{s,i}$ = inside surface area of shield

$\epsilon_{s,i}$ = emissivity of inside surface of shield

ϵ_w = mean emissivity of the two dissimilar metals used in the thermocouple

Using the above result, a thermocouple radiation heat transfer coefficient may be defined as:

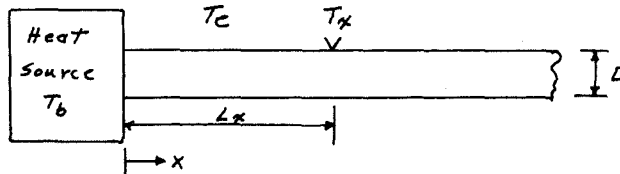
$$h_R = \frac{Q_R}{S_w T_0 \left(1 - \frac{T}{T_0} \right) (T_i - T_{s,i})} \quad (B-1.4)$$

APPENDIX C

BASE CONDUCTIVE HEAT TRANSFER

A. General Equations

Let us consider the general case of the heat transfer from a rod protruding from a heat source as shown below (Reference 16):



If we again neglect any radial temperature differences in the rod and consider the heat flow in an element dx of the rod, we obtain, as in Appendix A:

$$\frac{d^2 T_x}{dx^2} = m^2 (T_x - T_c) \quad \text{where } m^2 = \frac{hC}{KA}$$

which has the solution

$$(T_x - T_c) = c_1 e^{mx} + c_2 e^{-mx}$$

If the rod is very long in comparison with its diameter, we may use the boundary conditions:

$$T_x = T_b \quad \text{or } (T_x - T_c) = (T_b - T_c) \quad \text{at } x = 0$$

$$T_x = T_c \quad \text{or } (T_x - T_c) = 0 \quad \text{as } x \rightarrow \infty$$

Therefore

$$(T_x - T_c) = (T_b - T_c) e^{-mx}$$

Solving the above equation for the surface heat transfer coefficient

$$h_x = \frac{KD}{4(Lx)^2} \left\{ \ln \frac{T_b - T_c}{T_x - T_c} \right\}^2 \quad (C-1.0)$$

where:

- K = thermal conductivity of the rod
- D = diameter of rod
- T_b = temperature of heat source
- T_e = external environment temperature

Since the heat flow along the rod by conduction must be balanced by convection from the surface of the rod to the environment, we may write:

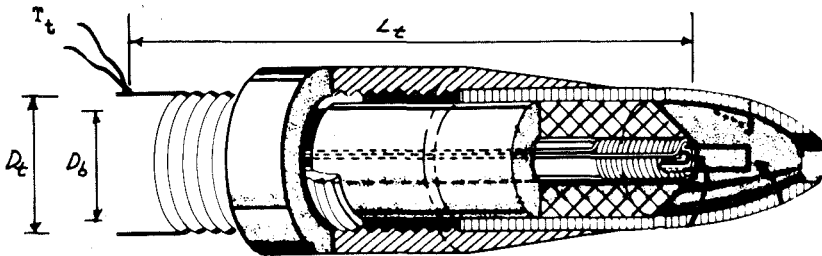
$$Q = -KA \frac{dT}{dx} \Big|_{x=0} = \int_0^{\infty} hC(T-T_e)dx$$

then

$$Q = -KA \left[-m(T_b - T_e) e^{-mx} \right]_{x=0} = \sqrt{hCKA} (T_b - T_e) \quad (C-1.1)$$

B. Specific Application

We may apply our general solution to the supporting tube of a temperature probe in the following manner:



Since the air around the tube is moving at a high speed, we shall assume an air surface temperature (T_{a_t}) equal to that obtained under adiabatic flow conditions. The surface to air convective heat transfer coefficient can then be obtained from:

$$h_t = \frac{K_t D_t}{4(L_t)^2} \left\{ \ln \frac{r_b - r_{ot}}{r_e - r_{ot}} \right\}^2 \quad (C-1.2)$$

$$K_t = \frac{K_b A_b + K_m A_m}{A_t}$$

where:

K_b = thermal conductivity of the thermocouple base holder

K_m = thermal conductivity of the metal support tube

and A_b and A_t are the cross-sectional areas of the base and metal tube respectively, in which $A_b + A_m = A_t$.

The heat transfer rate can then be expressed as:

$$Q_t = \frac{\pi}{2} \sqrt{K_t h_t D_t^3} T_o \left(1 - \frac{T}{T_o}\right) (T_b - T_{at}) \quad (C-1.3)$$

The above heat transfer rate can then be used to obtain a surface or film heat transfer coefficient of the base:

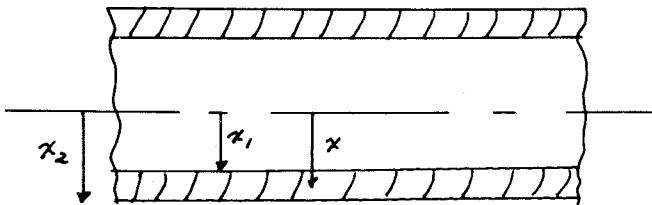
$$h_b = \frac{4 Q_t}{\pi D_b^2 T_o \left(1 - \frac{T}{T_o}\right) (T_c - T_b)} \quad (C-1.4)$$

APPENDIX D

SHIELD CONDUCTIVE HEAT TRANSFER

A. General Equations

The heat flow through flow through a body of circular cross section in which the direction of the flow is at all points radial and perpendicular to the axis is easily found from the basic, Fourier steady-state-thermal-conduction equation.



$$q = -k_s \frac{dT}{dr}$$

If the thermal conductivity is considered constant, and

$$\int_{r_1}^{r_2} \frac{dr}{r} = - \frac{k \pi L}{q} \int_{T_1}^{T_2} dT$$

or

$$q = - \frac{k \pi L (T_2 - T_1)}{\ln(r_2/r_1)}$$

If we use a mean value for the surface area (S_m), we can write:

$$q = - k S_m \frac{(T_2 - T_1)}{(r_2 - r_1)}$$

Then

$$S_m = \frac{S_2 - S_1}{\ln(S_2/S_1)}$$

$$q = -k \frac{(S_2 - S_1)}{\ln(S_2/S_1)} \frac{(T_2 - T_1)}{(r_2 - r_1)}$$

We can then write

$$h_{s_i} = \frac{d\dot{Q}_s / dS_{s_i}}{T_o \left(1 - \frac{T}{T_o}\right) (1 - r_{s_i})} \quad (D-11)$$

where:

- h_{s_i} = local inside shield convective heat transfer coefficient
- r_{s_i} = local inside shield recovery factor
- S_{s_i} = inside surface shield area $\approx S_m$

Since the Mach number of the flow within the shield is usually very low, the surface adiabatic recovery factor is assumed equal to one.

Using the above convective heat transfer coefficient, we may define a local internal Nusselts number

$$Nu_{s_i} = \frac{h_{s_i} x_{s_i}}{K_g}$$

where:

- $K_g = f(T_o)$ = air thermal conductivity
- x_{s_i} = distance from the entrance of the probe to location of T_{s_i} measurement

In forced convective heat transfer, the Nusselts number is related to the flow Reynolds number by an equation of the form

$$(Nu)_{s_i} = C_{s_i} Pr^a (Re)_{s_i}^b$$

where:

- Pr = Prandtl number = $\frac{c_p \mu}{K_g}$
- Re = Reynolds number = $\frac{\rho u l}{\mu}$
- C_{s_i} = experimental constant

For the heating or cooling of a fluid inside of a tube, Reference 27 indicates that an equation;

$$(Nu)_{s_i} = C_{s_i} Pr^{1/3} (Re^*)_{s_i}^{3/4} \quad (D-1.2)$$

should apply, where Re^* is a Reynolds number determined using the stagnation temperature for the evaluation of the gas density and viscosity, and with the characteristic length, X_{s_i} . Reference 32 indicates a better correlation of heat transfer data using the above definition of the Reynolds number.

If the temperature gradient through a point on the shield is known or can be estimated, the constant C_{s_i} can be determined. Using this constant and assuming the Reynolds number $(Re)_{s_i}^*$ to vary only with the distance from the shield entrance, we may estimate a Nusselts number for any point on the shield.

$$(Nu)_x = C_{s_i} Pr^{1/3} (Re^*)_{s_i}^{3/4} \left[\frac{(x_e - x)}{X_{s_i}} \right]^{3/4} \quad (D-1.3)$$

where:

$$(Nu)_x = \frac{(h_{s_i})_x (x_e - x)}{K_g} \quad (D-1.4)$$

in which, x_e = distance from base to entrance of shield where x is measured from the base of the probe as shown in the sketch.

The form of the equation requires the forced convective heat transfer coefficient to go to zero at the entrance to the shield.

The actual mean temperature of the shield is determined not only by the inside forced convection but also by the axial heat transfer along the shield itself. This is in turn affected by the heat transfer by radiation to the cool wind tunnel walls and by convection to the external

boundary layer from the outer surface of the shield. As a first approximation to this complex situation, we shall assume that the inside shield temperature varies linearly from a value of T_0 at the probe entrance to the value T_{si} as measured at a point X_{si} from the entrance. We may then write:

$$(1 - \gamma_{si})_{\kappa} = \alpha (x_e - x)$$

where

$$\alpha = \frac{(1 - \gamma_{si})_{\kappa_{si}}}{\kappa_{si}} \quad (D-1.5)$$

The total shield convective heat transfer can then be determined from:

$$Q_{ST} = \int_{x_b=0}^{x_e} dQ_s = \int_{x_b=0}^{x_e} (h_{s,\kappa})_{\kappa} (T_0) \left(1 - \frac{T}{T_0}\right) (1 - \gamma_{si})_{\kappa} dS_{si}$$

or

$$Q_{ST} = \alpha \pi T_0 \left(1 - \frac{T}{T_0}\right) \kappa_g \int_0^{x_e} (Nu)_{\kappa} D_x dx \quad (D-1.6)$$

where D_x = function of the geometry of the shield.

APPENDIX E

FABRICATION TECHNIQUE

As originally conceived, the research program envisioned operation of the stagnation temperature probe at high supersonic speeds, $M = 6$ to 9 , and stagnation temperatures of 200 to 1200°F . Operation at these elevated temperatures presented a severe material and fabrication problem. In general, the problem was met by the use of glass, quartz, and ceramic materials and ceramic base cements.

Several of the probe shields were made of "Vycor", which is a 96 per cent silica glass made by the Corning Glass Works. The characteristics of this glass and several other materials used are presented in Table I. Since the Vycor, as purchased, did not have the desired thickness or internal diameter, it was necessary to have the tube drawn to the correct dimensions. This process was performed by the T. H. Garner Company of Claremont, California.

A carbon mandrel, accurately machined to the desired shield internal contour, was inserted in the drawn tubing and the open end drawn down to a narrow tip and sealed off. The other end of the tubing was connected to a vacuum pump. Starting at the tip, the tube was heated until it collapsed around the mandrel. Upon cooling, the mandrel could usually be removed without difficulty. This portion of the work was performed by Mr. Fred Wild, the CIT campus glassblower. The tip and external surface were then cut, ground, and polished to the desired dimensions. This operation proved to be a very difficult step and was performed by the Mindrum Precision Products Company of Cucamonga, California.

The small vent-holes in the shield were ground in the shield by means of small stainless tubing with a diamond lapping compound Grade No. 45 with a grit size of 325 mesh using water as a lubricant. The tip of the stainless tubing was annealed before use.

Considerable study was also made of the use of a zirconia base ceramic as a shield material. In this case, the material was sprayed on to a polished stainless steel mandrel of the internal shield contour. The process used was that of the Metallizing Engineering Co., and involved their Thermo Spray Gun and Thermo Spray Powder No. 201. The hot material is sprayed on in one continuous operation, until the approximate thickness is obtained. In our case this thickness was .025 inches. The large difference in the coefficient of thermal expansion between the two materials usually allowed the two to be separated when cooled. If the shield stuck to the mandrel, liquid air was used to cool the stainless material and the shield was tapped off. Since the ceramic is quite soft at this state the vent holes, tip, and external surface were drilled and hand ground. The final operation was to coat the shield with a glass glaze (Frit PB 742-900; E.P.K.-100; Boric Acid-10) similar to that used on fine china made by the B. F. Wagner Co. The glaze was diluted with water, painted on, and fired at 1550°F. The ceramic material was, in the end, found to be much easier to work with than the glass and has the advantage that it can be formed into almost any contour since the mandrel can, if necessary, be etched away with acid.

The base of the probe was made of fused silica (quartz) from thick wall tubing purchased from the Amersil Company. The outside diameter and exposed end were ground and polished by the Mindrum Company.

As a final step, the entire shield and exposed end of the base were painted with either Liquid Bright Platinum #05-x or Liquid Bright Gold No. 4942

and fired at a temperature of 1180°F. The platinum was found to adhere better and tarnish less than the gold.

The small heater elements used in two of the probes were made from 0.003-inch nichrome V wire. In the case of the base heater, the wire was carefully coiled around a small glass tube and then coated with high temperature varnish. The base and indicating thermocouples were stripped of the fiberglass insulation and in turn cemented around a still smaller glass tube with the varnish. This tube was then positioned and cemented with a filler type cement (either No. 29 Sauereisen or technical "B" copper cement) into the heater element tube, which was in turn cemented into the quartz base.

The nichrome wire was cemented onto the shield by positioning the shield vertically. The loose coils were held onto the shield with tiny pieces of masking tape and, while working towards the tip, each coil was cemented into position with No. 185 Adweld cement. This cement will disintegrate at temperatures over about 600°F, but it has since been found that if the wires can be held in position, the glass glaze acts as a very effective high temperature cement.

The indicating thermocouple was made by butt welding the iron and constantan wire and then hand filing and polishing the junction until it was again round and invisible to the naked eye.

The success of the various techniques discussed above can be attributed completely to the skill and persistence of Mr. C. A. Bartsch and Mr. Howard McDonald of the Aeronautical Machine Shop who were able to manufacture the probes to a high degree of accuracy.

A list of names and addresses of suppliers of essential items is given below:

Precision Drawn Glass and Quartz

T. H. Garner Co.
177 South Alexander Avenue
Claremont, California

Mindrum Precision Products
8024 Archibald Avenue
Cucamonga, California

Fused Quartz

Amersil Company, Inc.
685 Ramsey Avenue
Hillside, New Jersey

Vycor Glass

Braun Chemical Company
1363 South Bonnie Beach Place
Los Angeles 54, California

Corning Glass Works
Technical Products Division
Corning, New York

Stainless Tubing

Tubesaes
2211 Tubeway
Los Angeles 22, California

Thermocouple Wire

Leeds and Northrup Company
5111 Via Corona Avenue
Los Angeles 22, California

Angus-Campbell, Inc.
4417 South Soto Street
Los Angeles 58, California

Thermo Electric Company
c/o S. R. Brown Company
14544 Archwood Street
Van Nuys, California

Very Fine Wire

Sigmund Cohn Corp.
121 South Columbus Avenue
Mt. Vernon, New York

Ceramic Coated Wire

Sequoia Wire and Cable Co.
2201 Bay Road
Redwood City, California

Hi Temp. Wire Corp.
1200 Shanes Drive
West Berry, Long Island
New York

Ceramic Cements

W. V-B Ames Company
Fremont, Ohio

Sauerisen Cements Company
Pittsburgh 15, Penn.

Nichrome Wire

Driver - Harris Company
Harrison, New Jersey

Ceramic Sprays

Metallizing Engineering Co.
Westbury, Long Island
New York

Glass Glaze

B. F. Wagner Co.
186 N. Vernon Ave.
Pasadena, California

Gold and Platinum

Hanovia Chemical and Mfg. Co.
East Newark, N. J.

E. I. Du Pont
Electrochemical Department
Wilmington, Delaware

Adweld Cement

Miracle Adhesives Corp.
New York 22, New York

TABLE I

Properties of Probe Materials

Physical Property	VYCOR No. 7900	Fused Quartz	Zirconia Ceramic
Softening Point	1500°C	1600-1700°C	-
Maximum Operating Temperature	900°C	1000°C	-
Melting Point	-	-	4600° F
Density (gm/cm^3)	2.18	2.20	5.2 to 5.3
Porosity (percent)	0	0	6 to 10
Coeff. of Expansion	$8.0 \times 10^{-7} / ^\circ\text{C}$	$5.5 \times 10^{-7} / ^\circ\text{C}$	$6.4 \times 10^{-6} / ^\circ\text{F}$
Dielectric Constant at 20° C	3.8	3.8	-
Thermal Conductivity	See Figure 4.		

TABLE II

Physical Properties and Parameters of
Base and Shield Heated Probe

D_w	=	.01	inches	A_p/A_e	=	6.25
D_e	=	.08	inches	A_{s1}	=	.120 in ²
D_b	=	.20	inches	A_e/A_v	=	6.0
D_t	=	.25	inches	L/D_w	=	20
L_t	=	1.05	inches	C_D	=	.988
t_s	=	.025	inches	K_w	=	.0006
x_{s1}	=	.16	inches	K_T	=	.00009
x_e	=	.23	inches	K_b	=	.000029
ϵ_w	=	.06		K_s	=	.000021
ϵ_s	=	.932				

$$D_x = 0.20 \sqrt{1 - 16x^2}$$

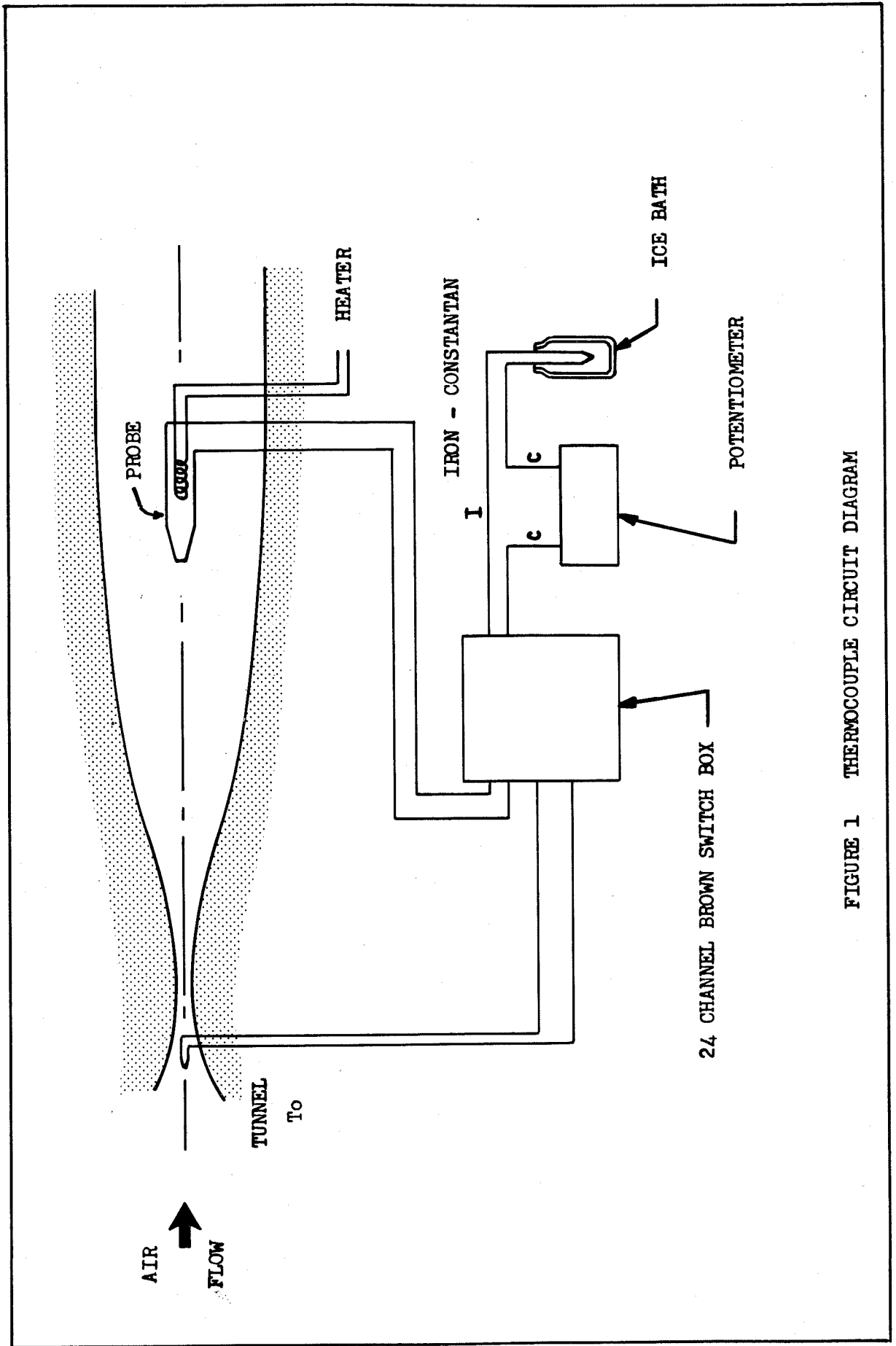


FIGURE 1 THERMOCOUPLE CIRCUIT DIAGRAM

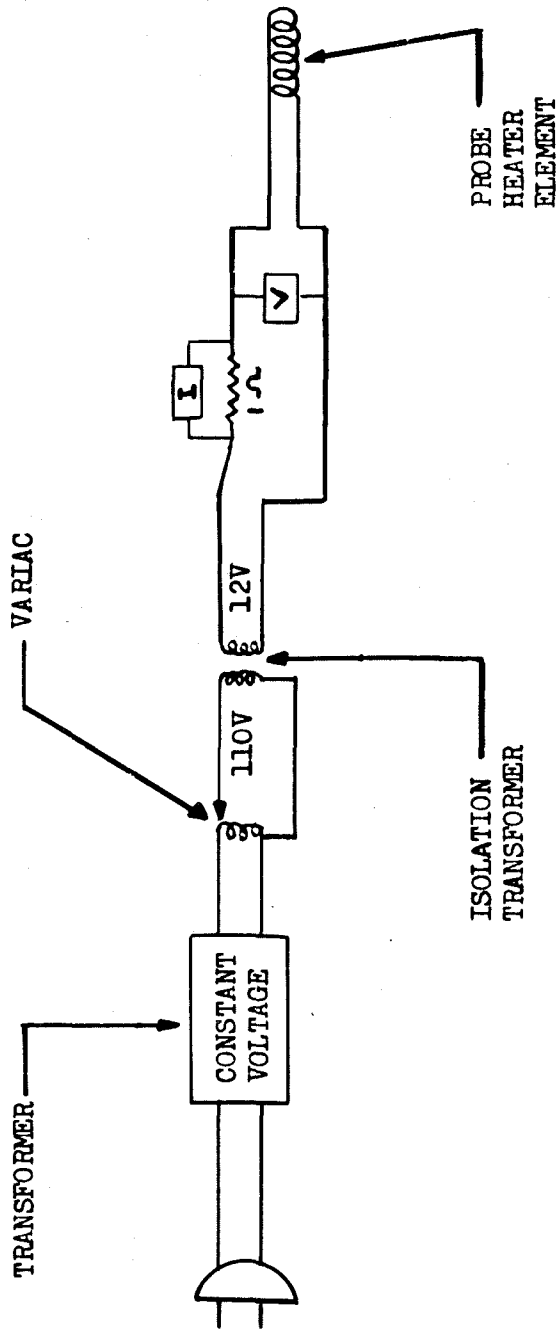
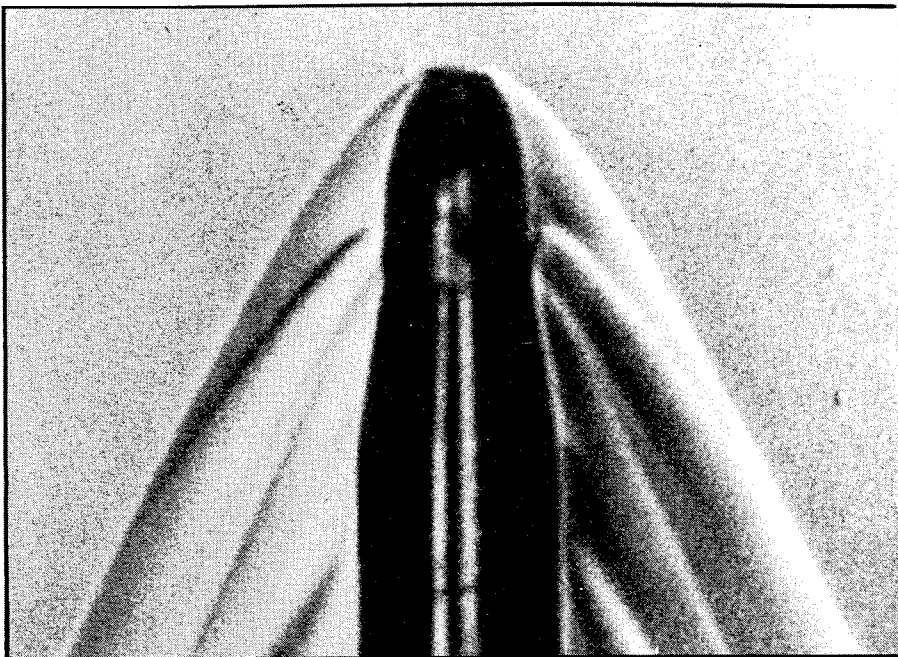


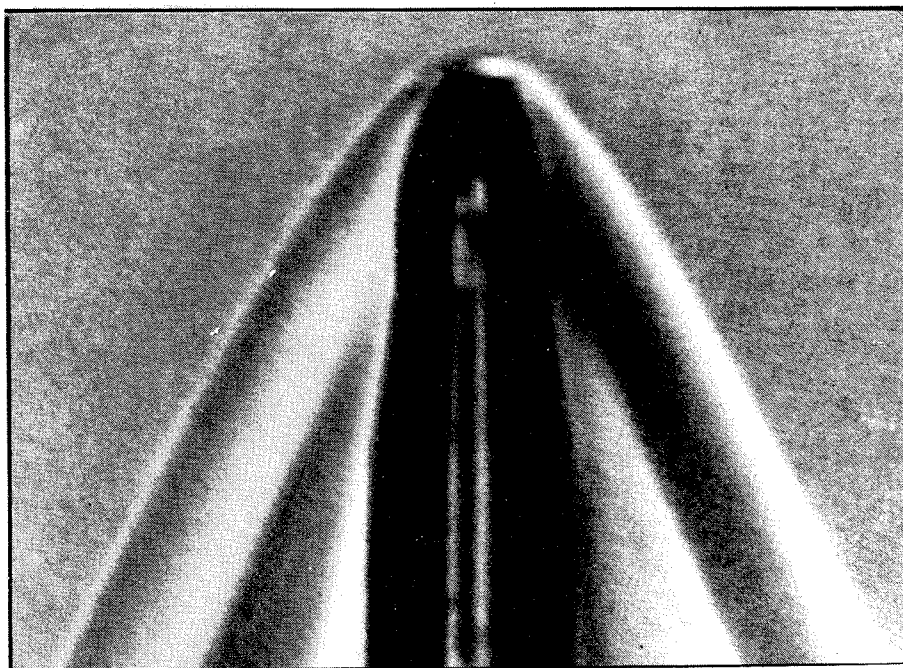
FIGURE 2 PROBE HEATER CIRCUIT DIAGRAM



$M = 2.81$

$Av/Ae = 1.0$

$Re = 4.67 \times 10^4$



$Av/Ae = 0$

FIGURE 3 SCHLIEREN PHOTOGRAPHS OF BASE HEATED STAGNATION TEMPERATURE PROBE

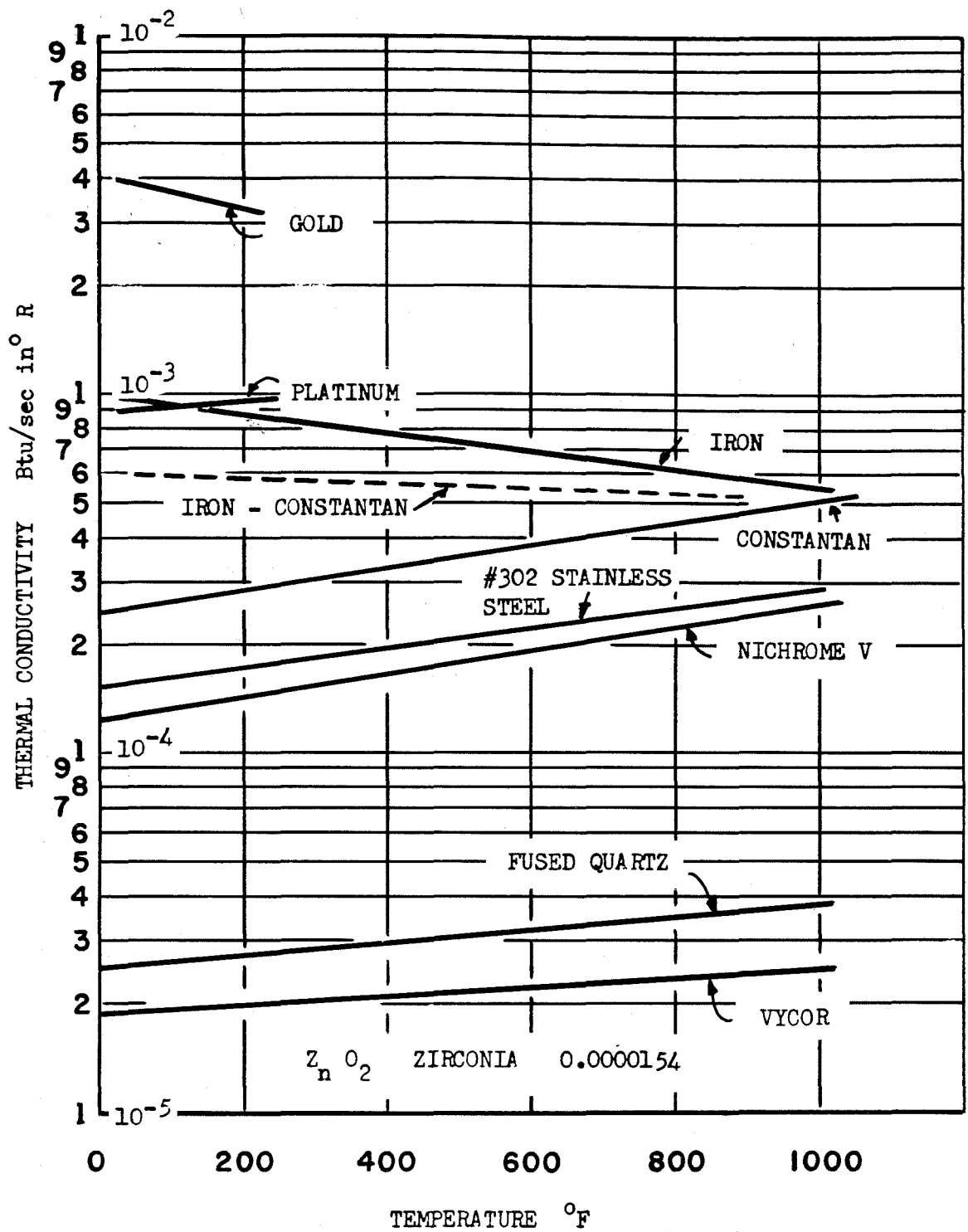
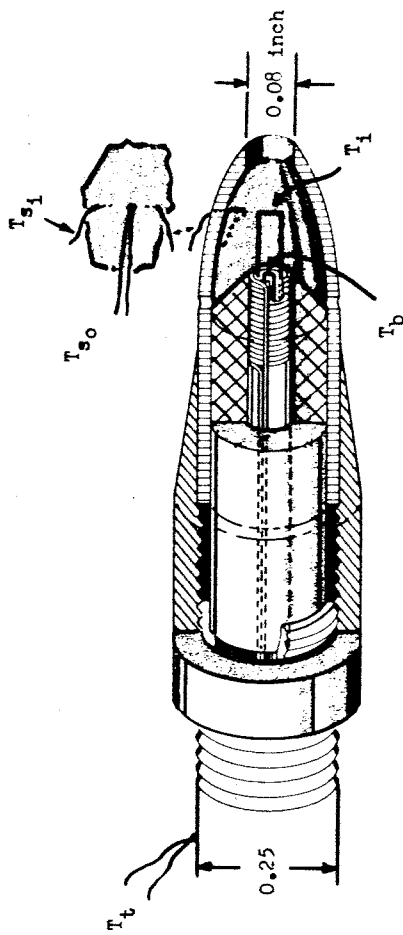
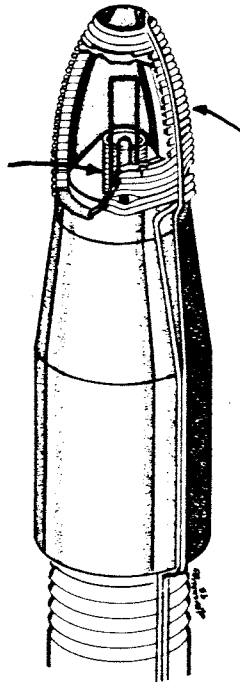


FIGURE 4 THERMAL CONDUCTIVITY OF PROBE MATERIALS

- T - Free stream temperature
- T_i - Indicated temperature
- T_b - Base temperature
- T_{s_1} - Shield inside temperature
- T_{s_0} - Shield outside temperature
- T_t - Supporting tube temperature






Nichrome base heater

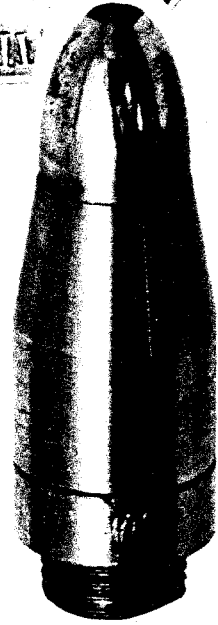


Nichrome shield heater

Exposed surfaces gold plated

Thermocouples: Iron-constantan

-  Quartz base
-  Vycor shield
-  Stainless steel holder and tube



BASE HEATED

Figure 5 Base and Shield Heated Stagnation Temperature Probe

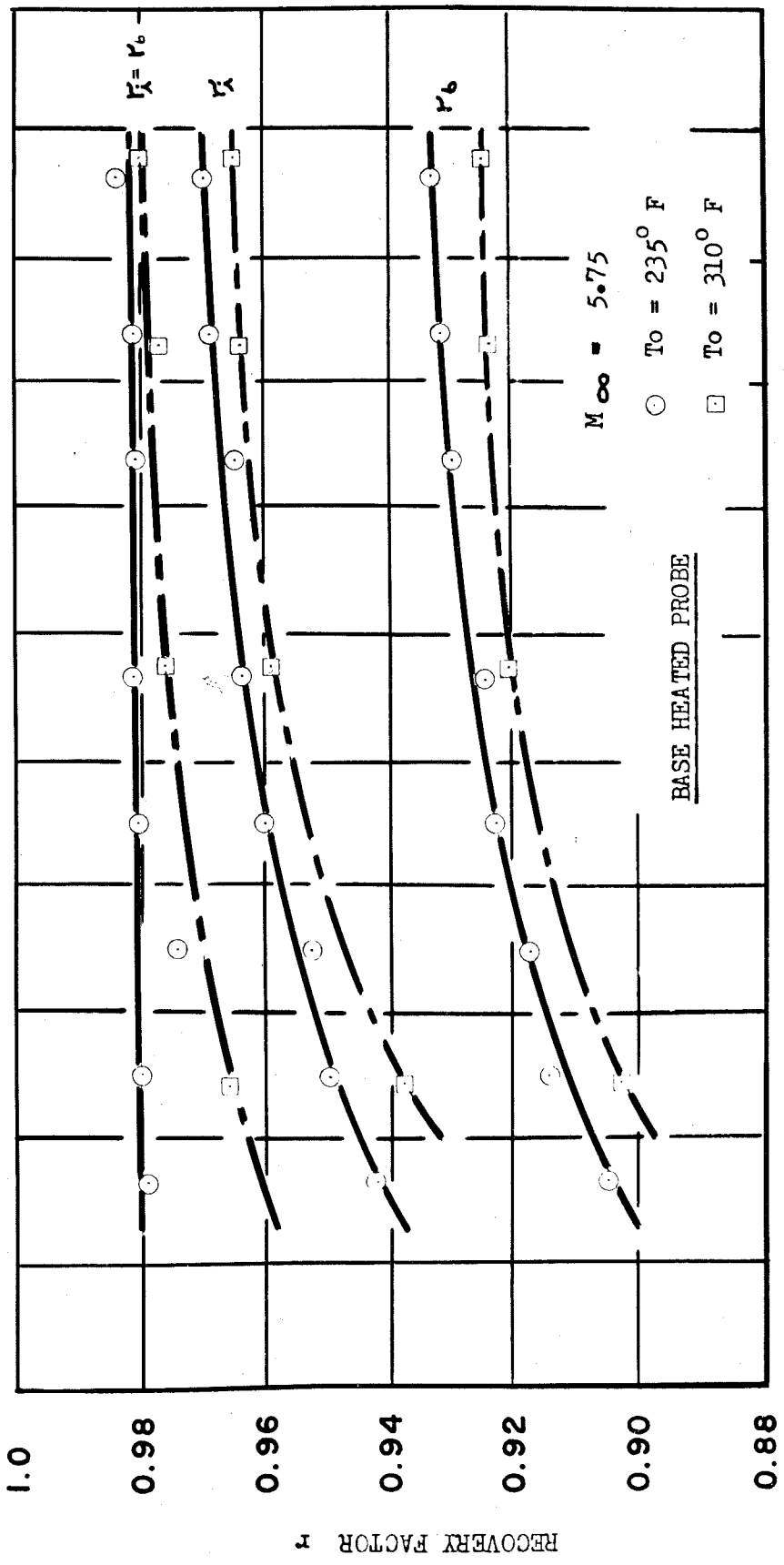


FIGURE 6 RECOVERY FACTOR VERSUS FREE STREAM REYNOLDS NUMBER AT TWO STAGNATION TEMPERATURES

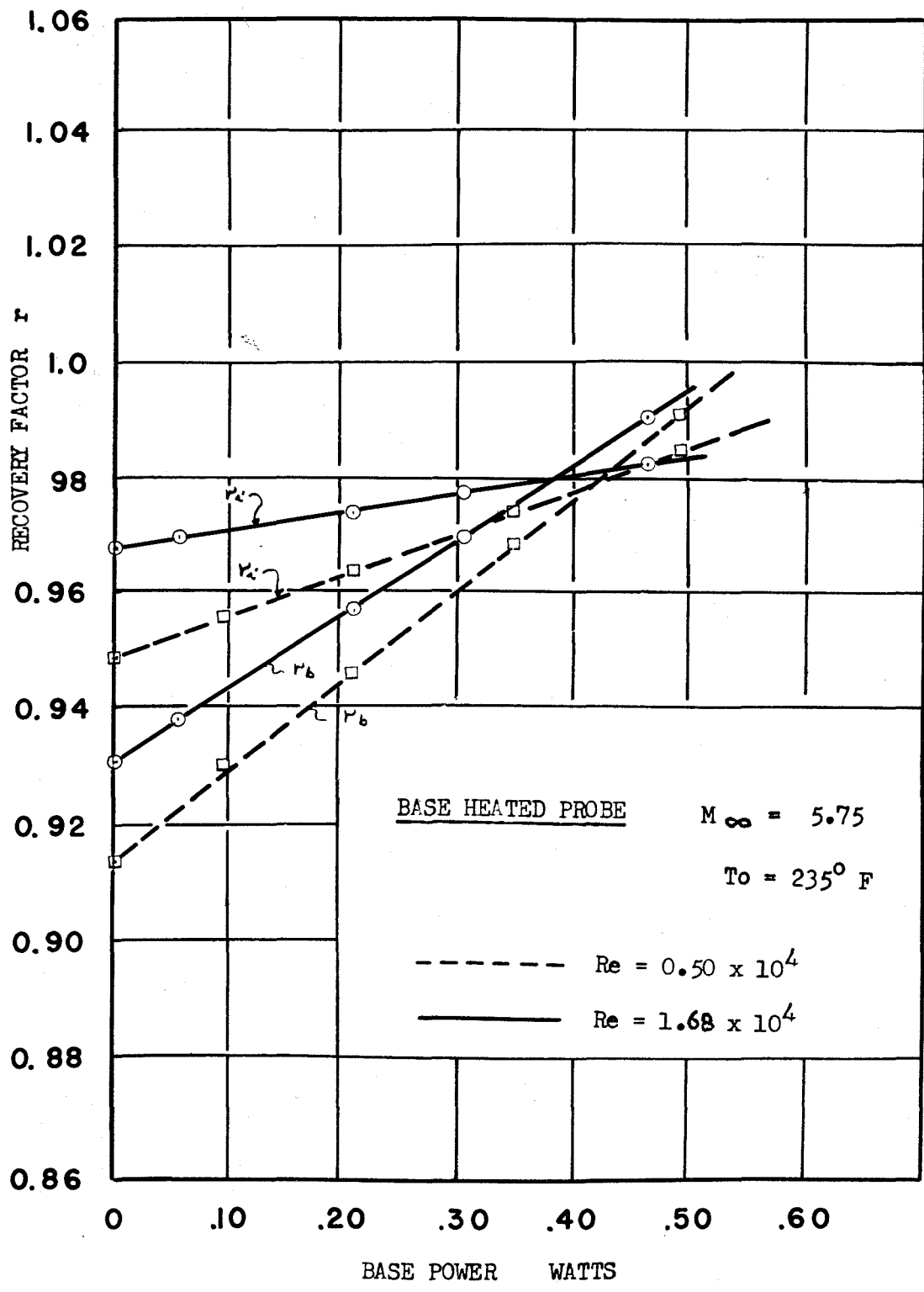


FIGURE 7 RECOVERY FACTOR VERSUS BASE POWER

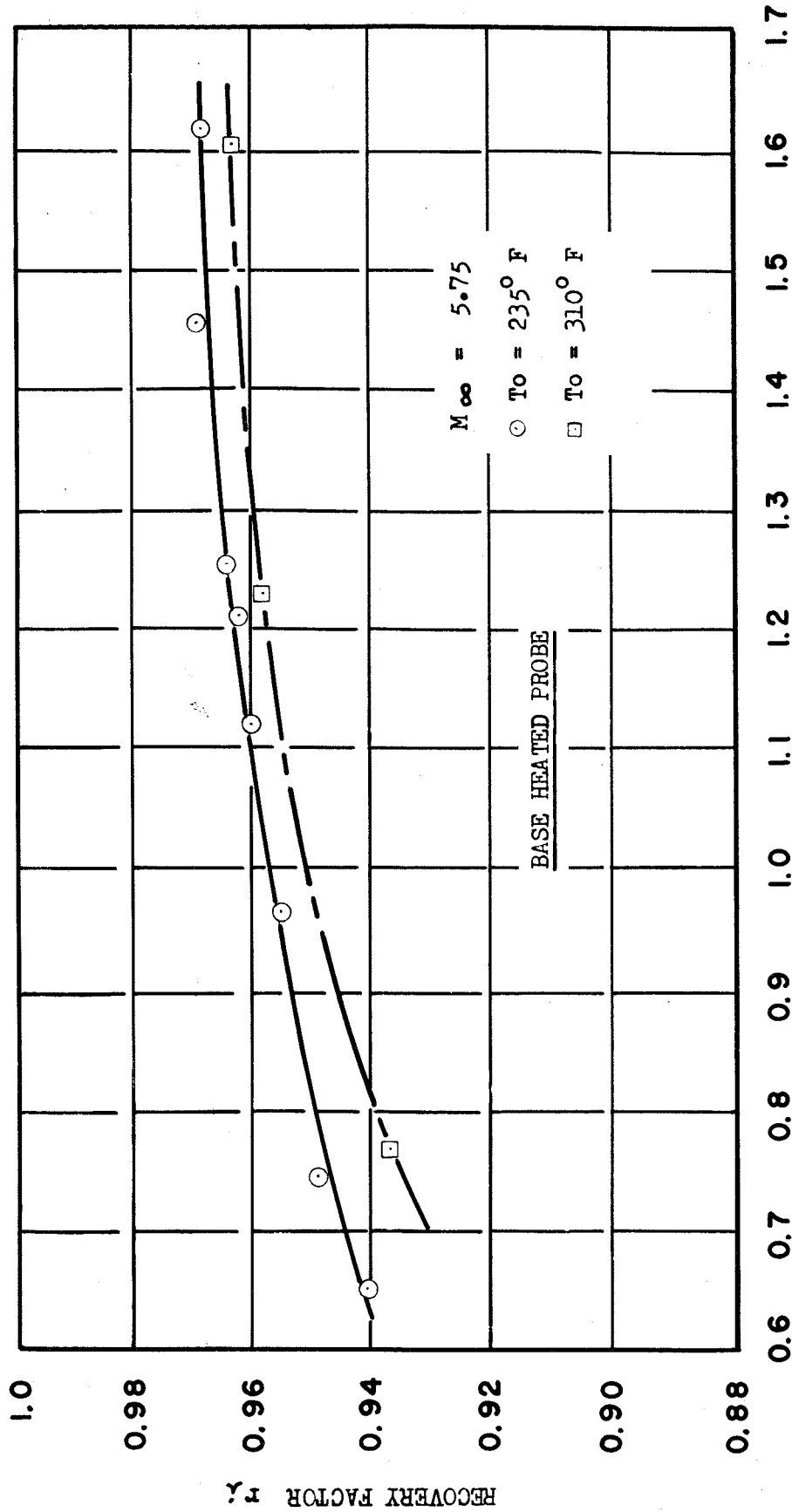
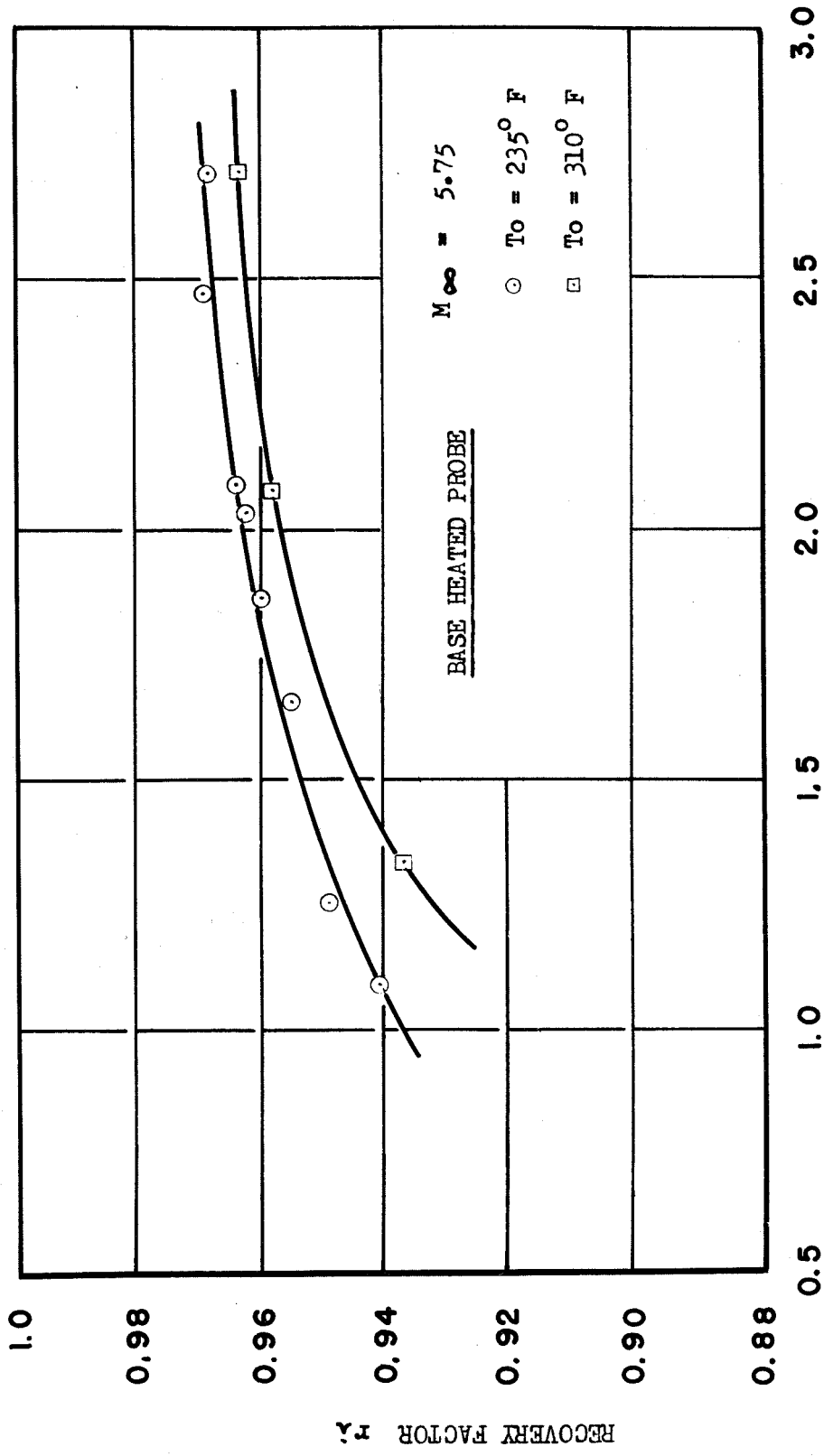


FIGURE 8 RECOVERY FACTOR VERSUS THERMOCOUPLE CONVECTIVE HEAT TRANSFER COEFFICIENT FOR TWO STAGNATION TEMPERATURES



$Nu_w \frac{k_g}{k_w} \times 10^3$

RECOVERY FACTOR VERSUS FACTOR $(Nu_w \frac{k_g}{k_w})$

FIGURE 9

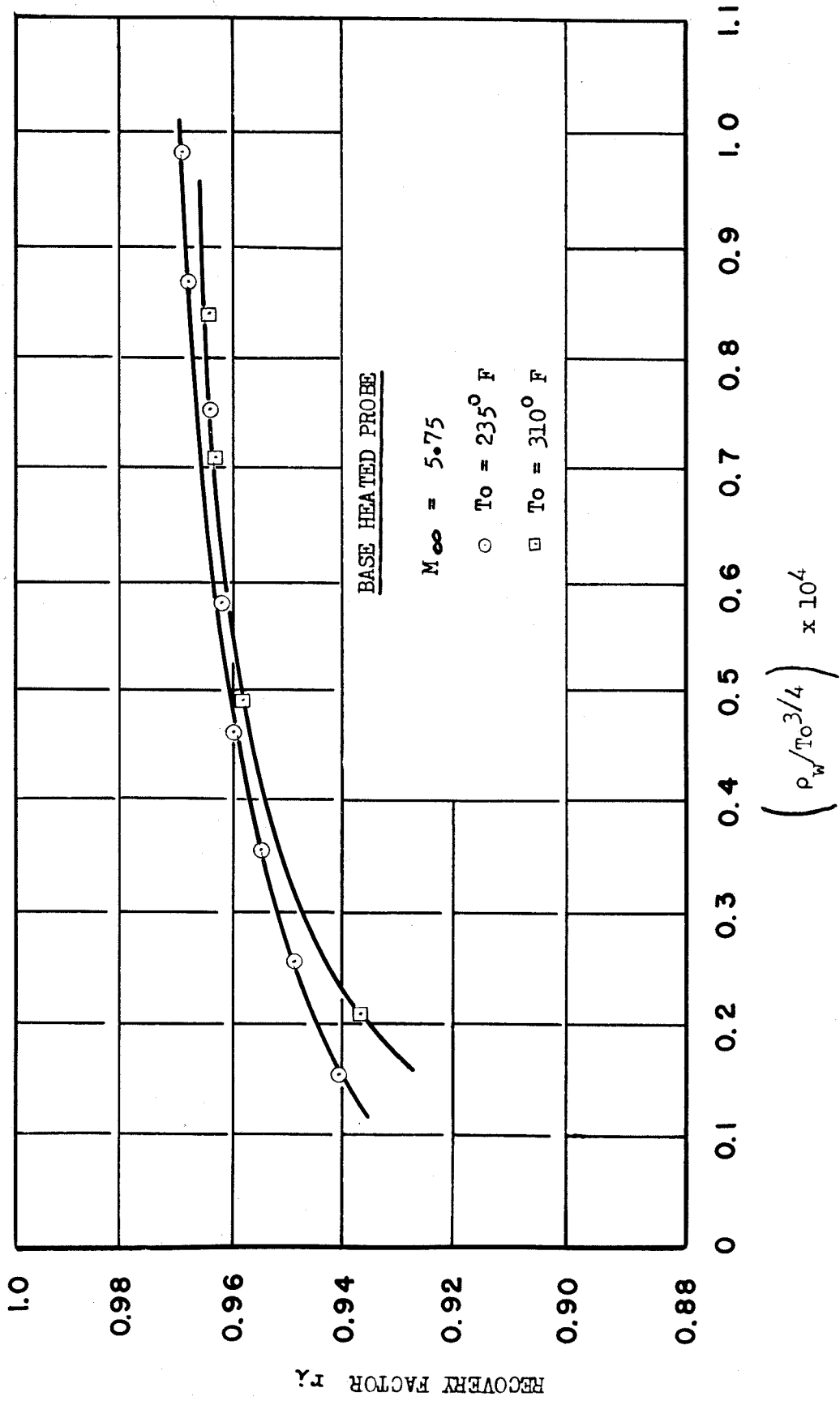


FIGURE 10 RECOVERY FACTOR VERSUS FACTOR $(P_w/T_o^{3/4})$

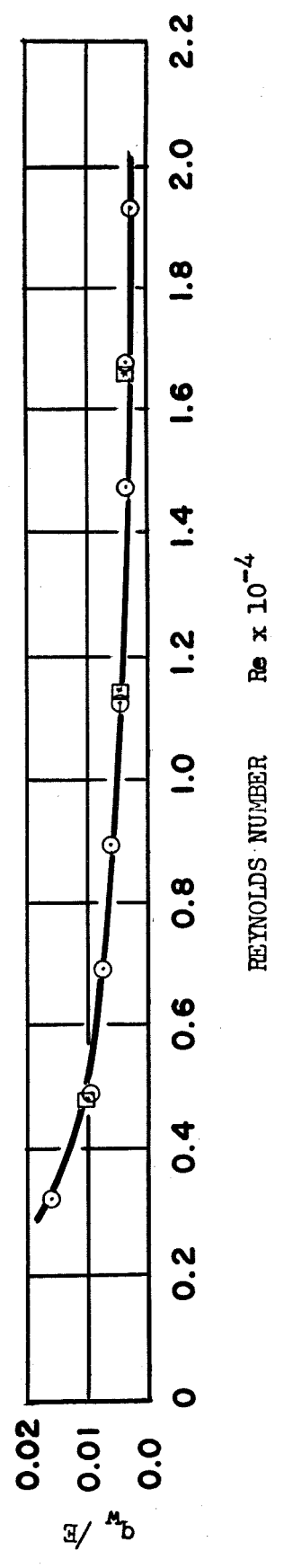
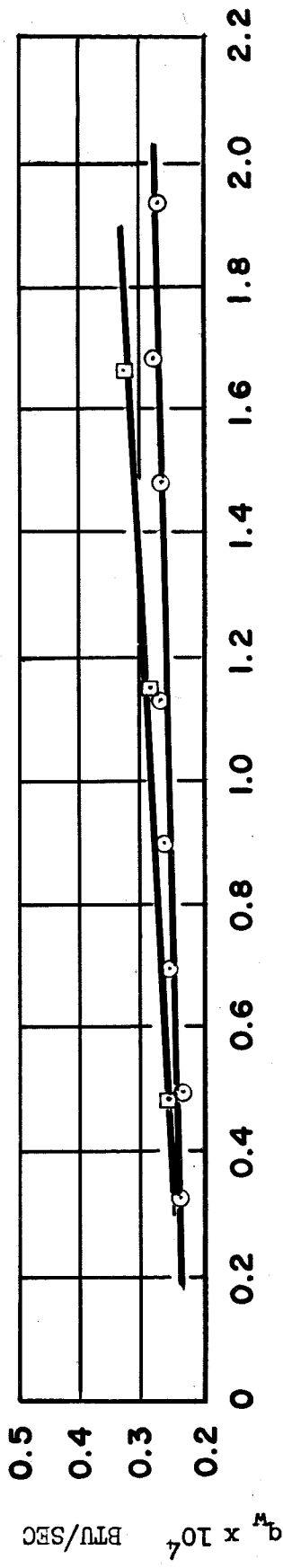
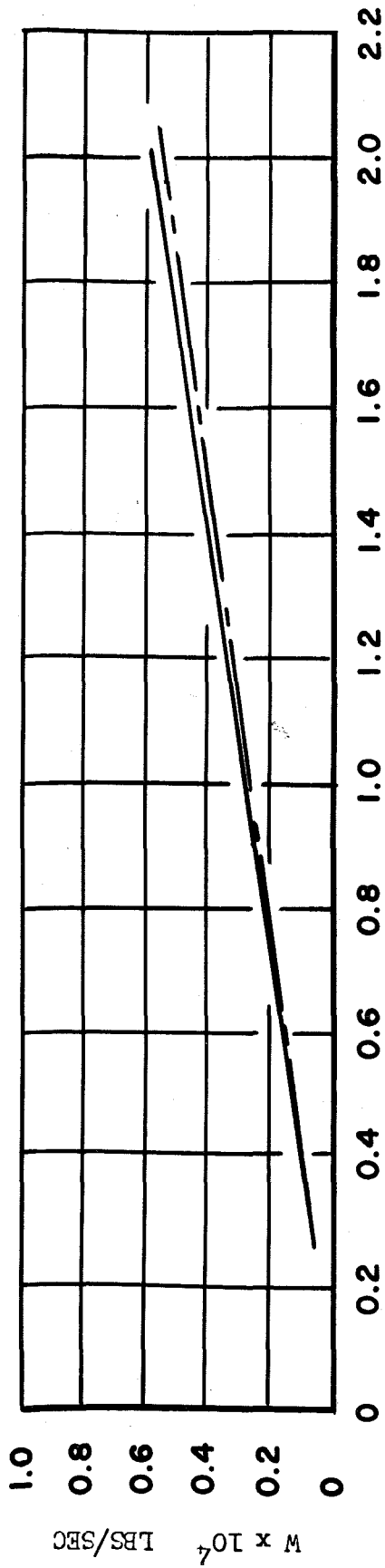


FIGURE 11 THERMOCOUPLE CONDUCTION HEAT TRANSFER VERSUS FREE STREAM REYNOLDS NUMBER AT $M_\infty = 5.75$



BASE HEATED PROBE

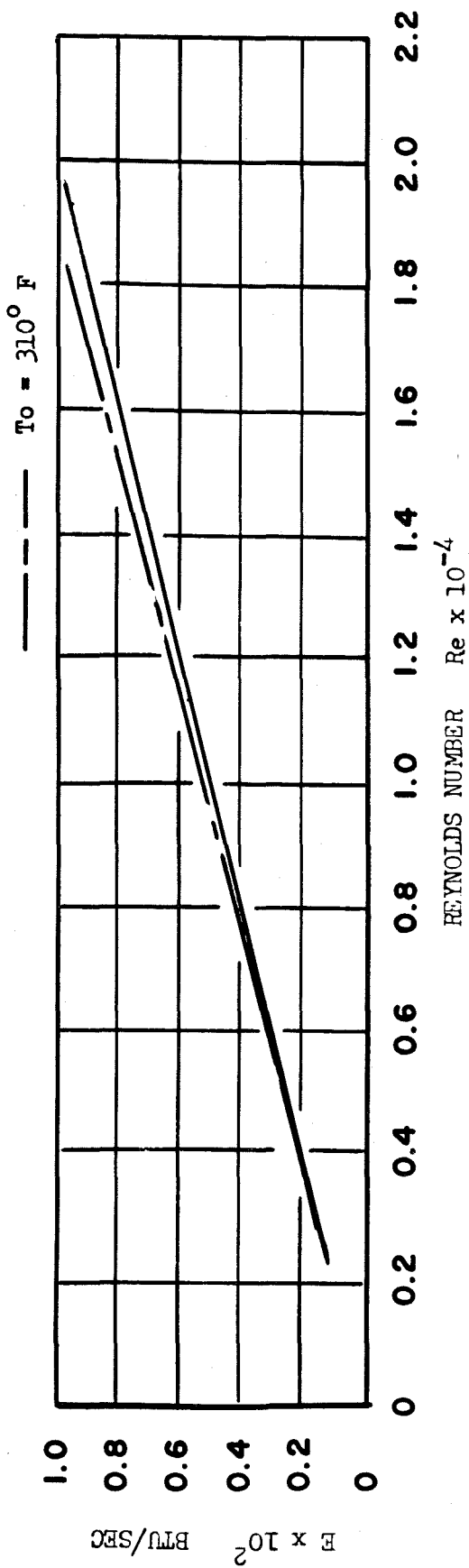


FIGURE 12 PROBE MASS AND ENERGY FLOW RATE VERSUS FREE STREAM REYNOLDS NUMBER AT $M_\infty = 5.75$

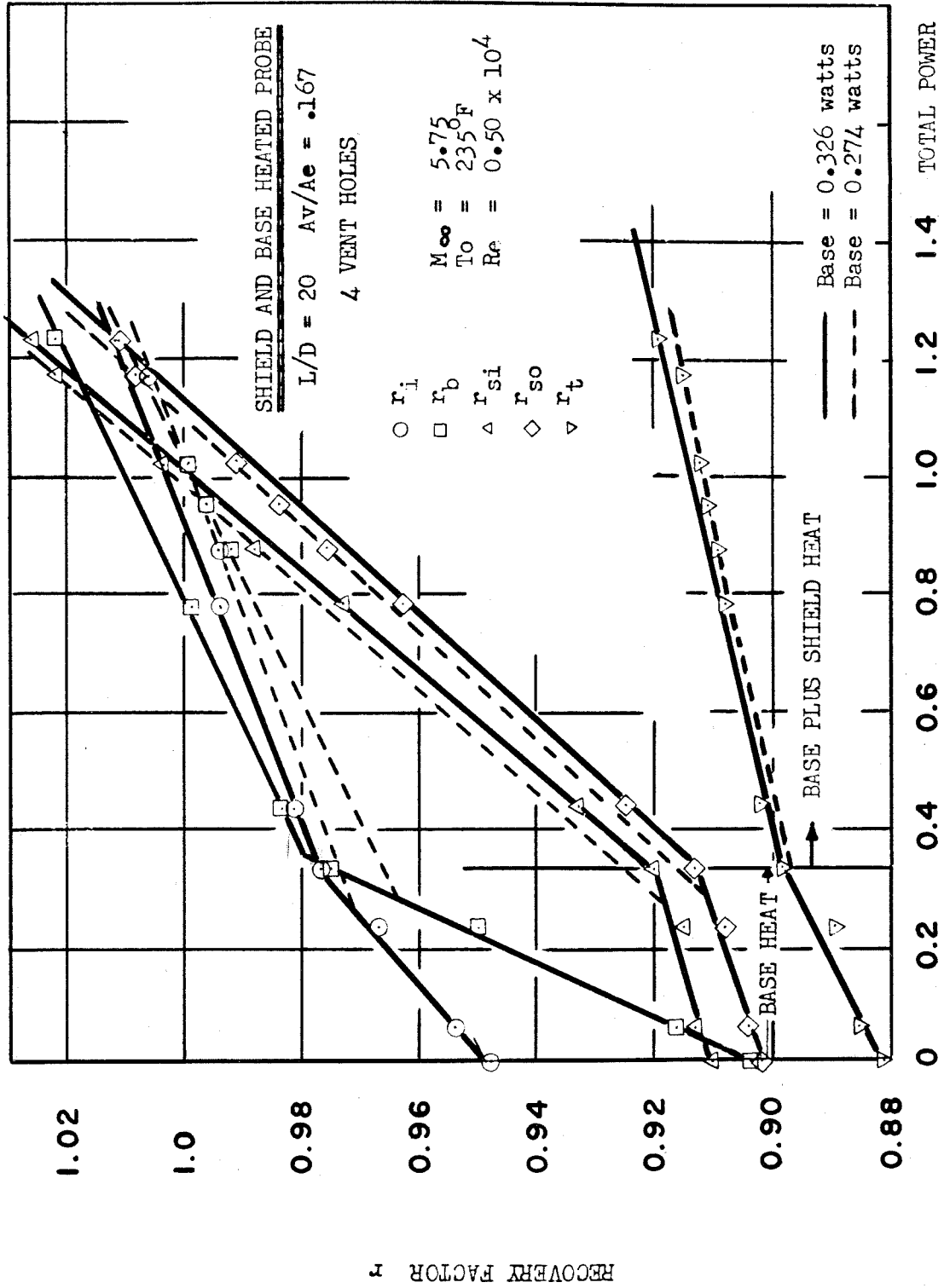


FIGURE 13 Recovery Factors Versus Base and Shield Power at $T_o = 235^\circ F$

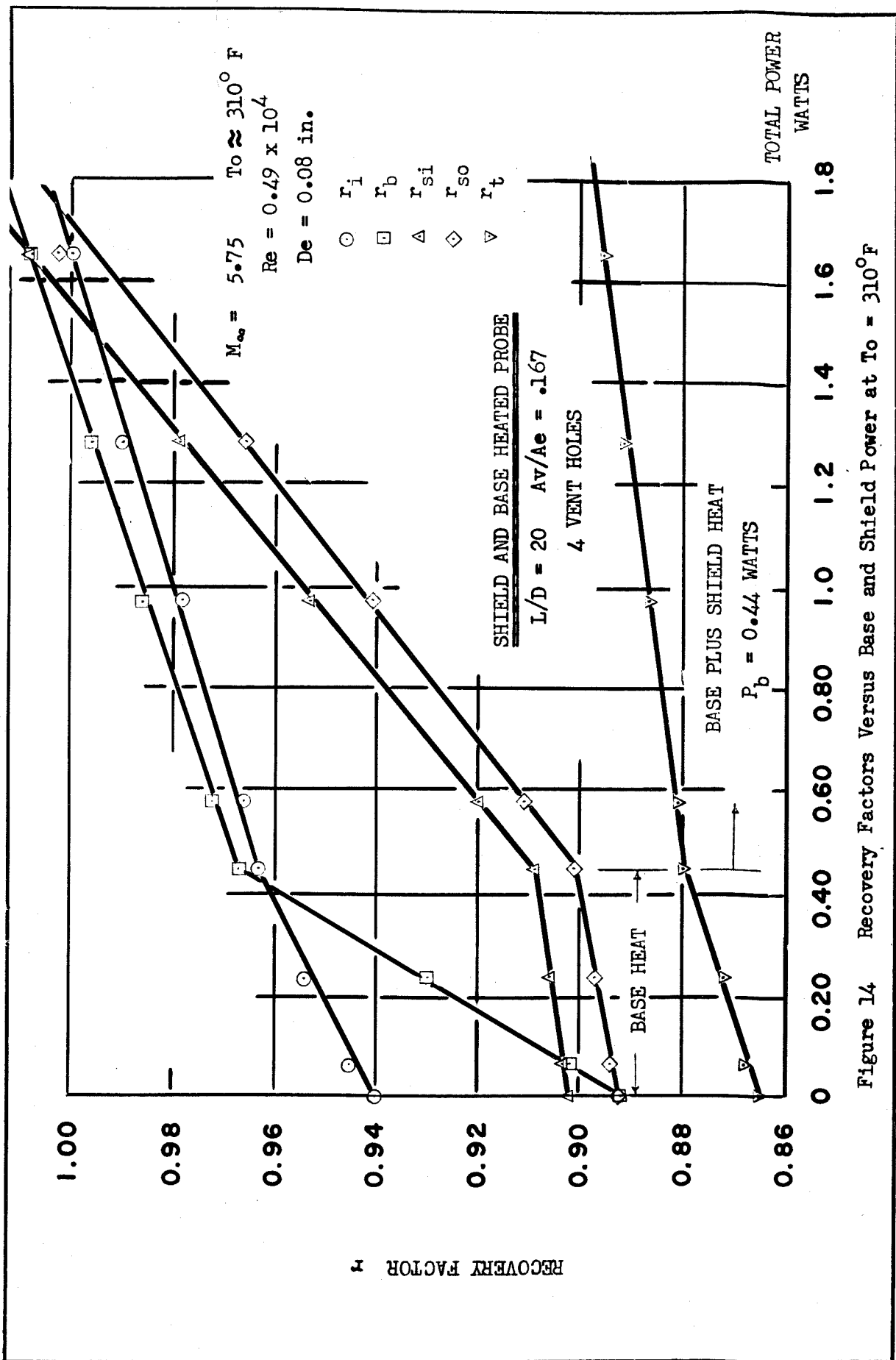


Figure 14 Recovery Factors Versus Base and Shield Power at $T_o = 310^\circ \text{F}$

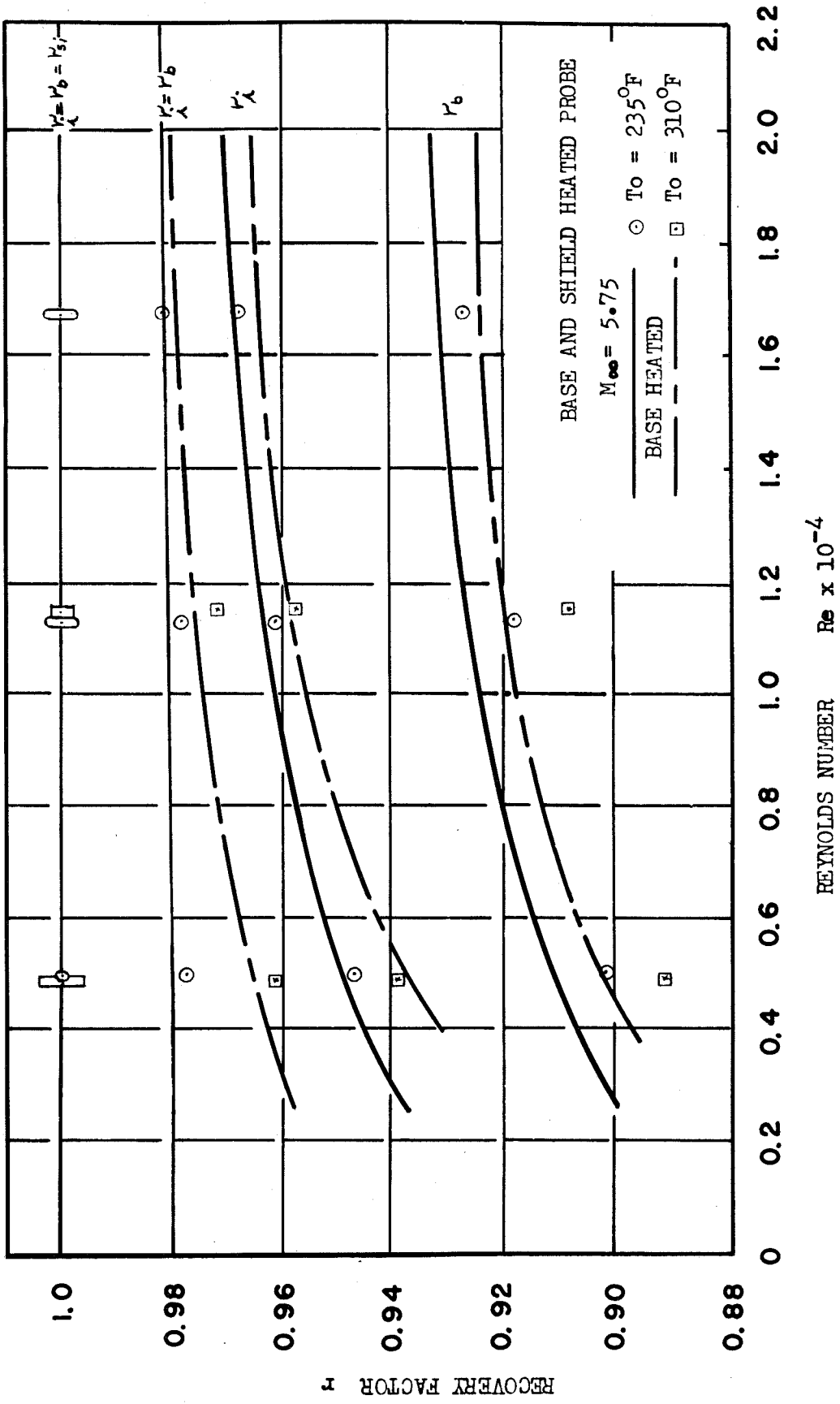


Figure 15 RECOVERY FACTOR VERSUS FREE STREAM REYNOLDS NUMBER FOR BASE AND SHIELD PROBE AT $M_{\infty} = 5.75$

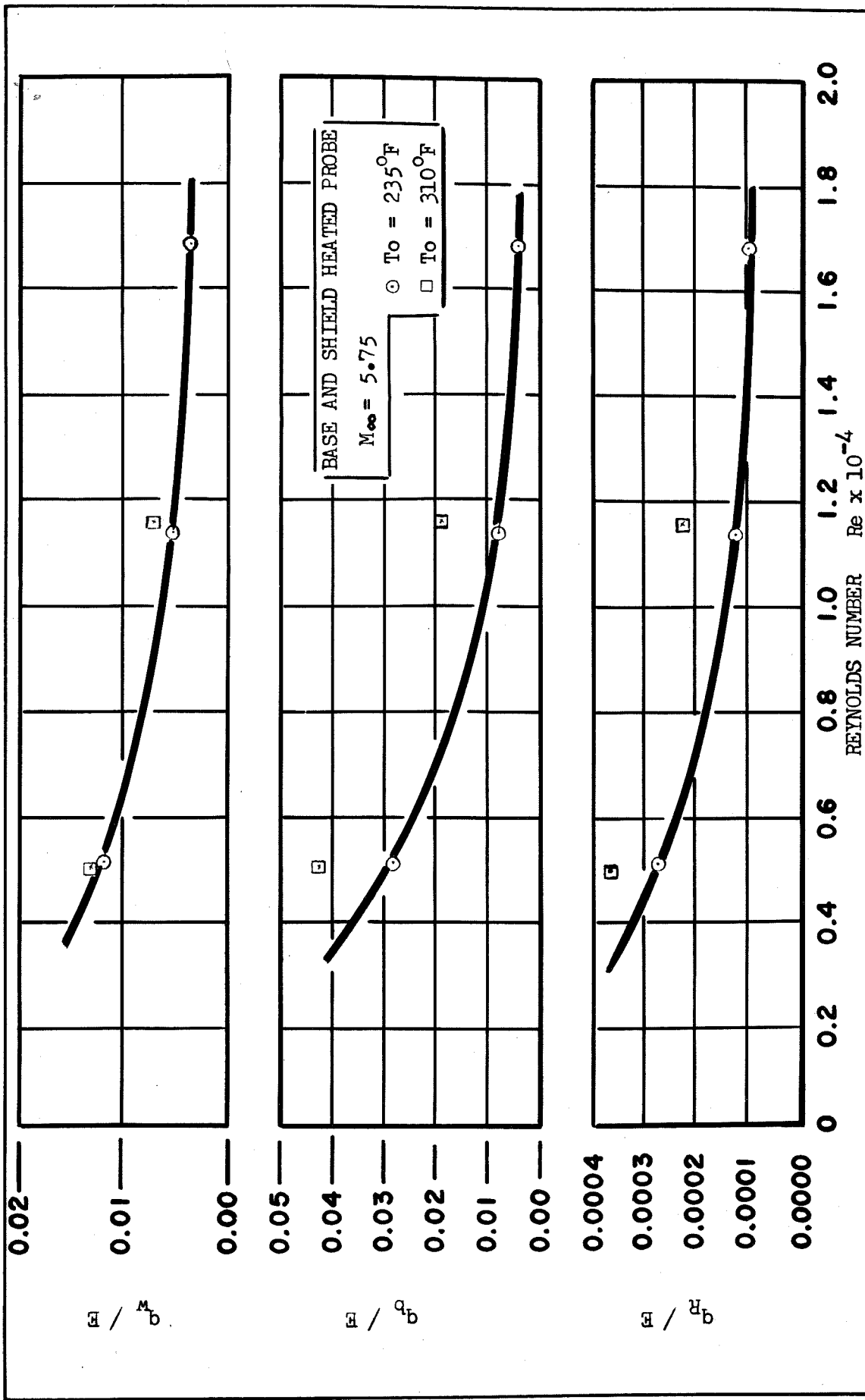


FIGURE 16 LOSS RATIOS VERSUS FREE STREAM REYNOLDS NUMBER FOR BASE AND SHIELDED HEATED PROBE (Continued)

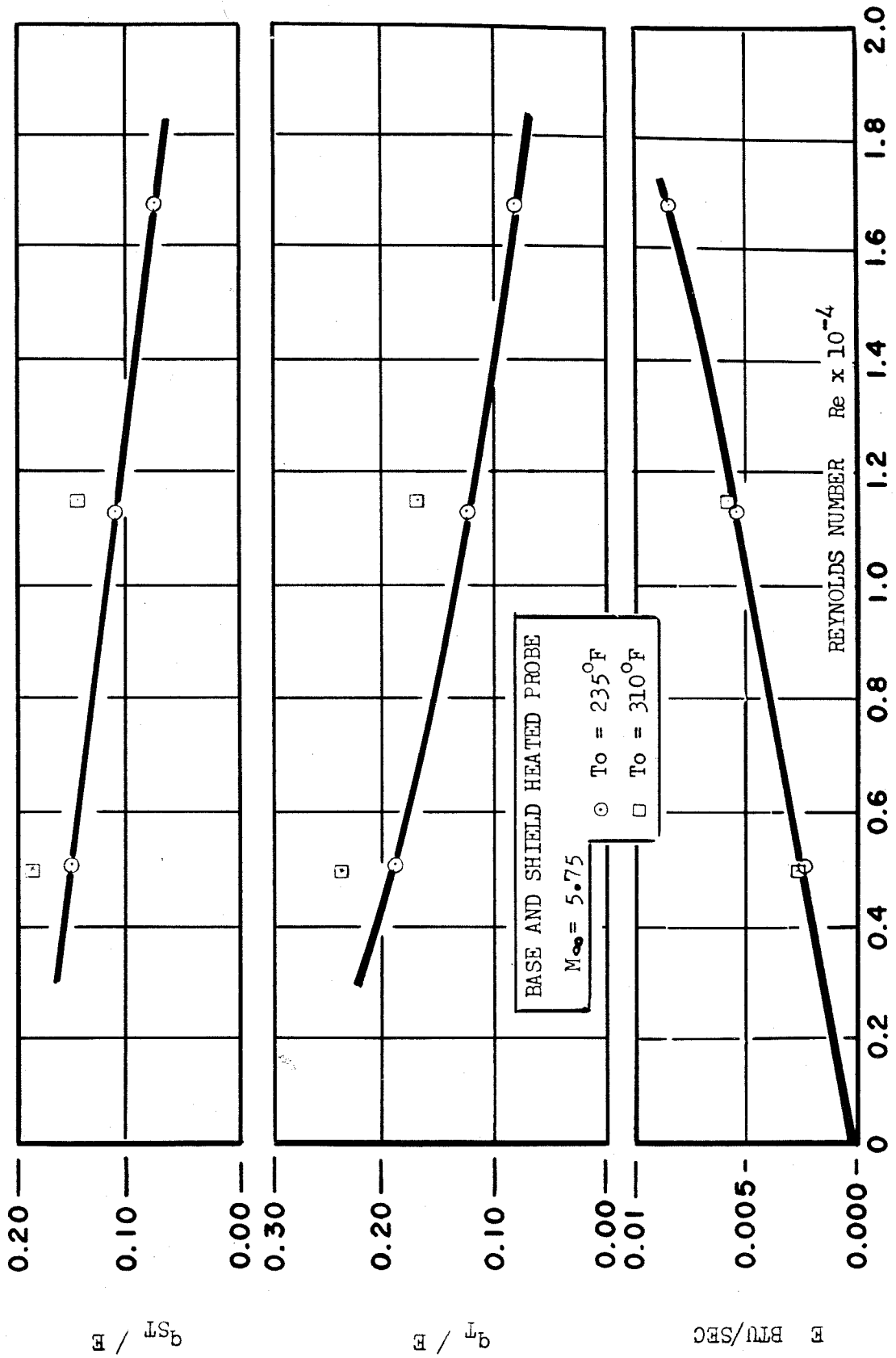


FIGURE 16 (Continued) LOSS RATIOS VERSUS FREE STREAM REYNOLDS NUMBER FOR BASE AND SHIELDED HEATED PROBE

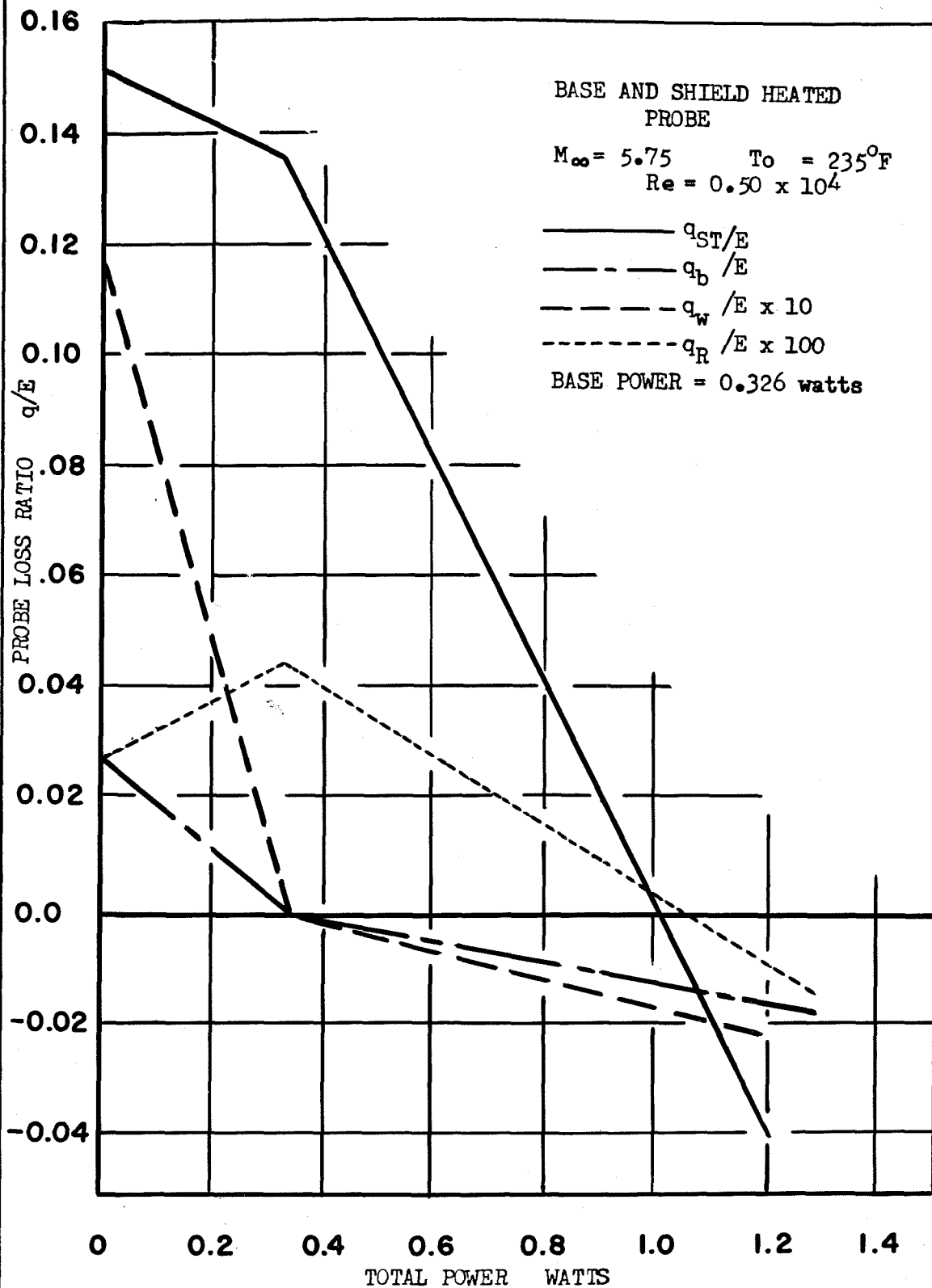


FIGURE 17 PROBE LOSS RATIO VERSUS TOTAL POWER SUPPLIED FOR
BASE AND SHIELD HEATED PROBE $P_b = 0.326$ WATTS

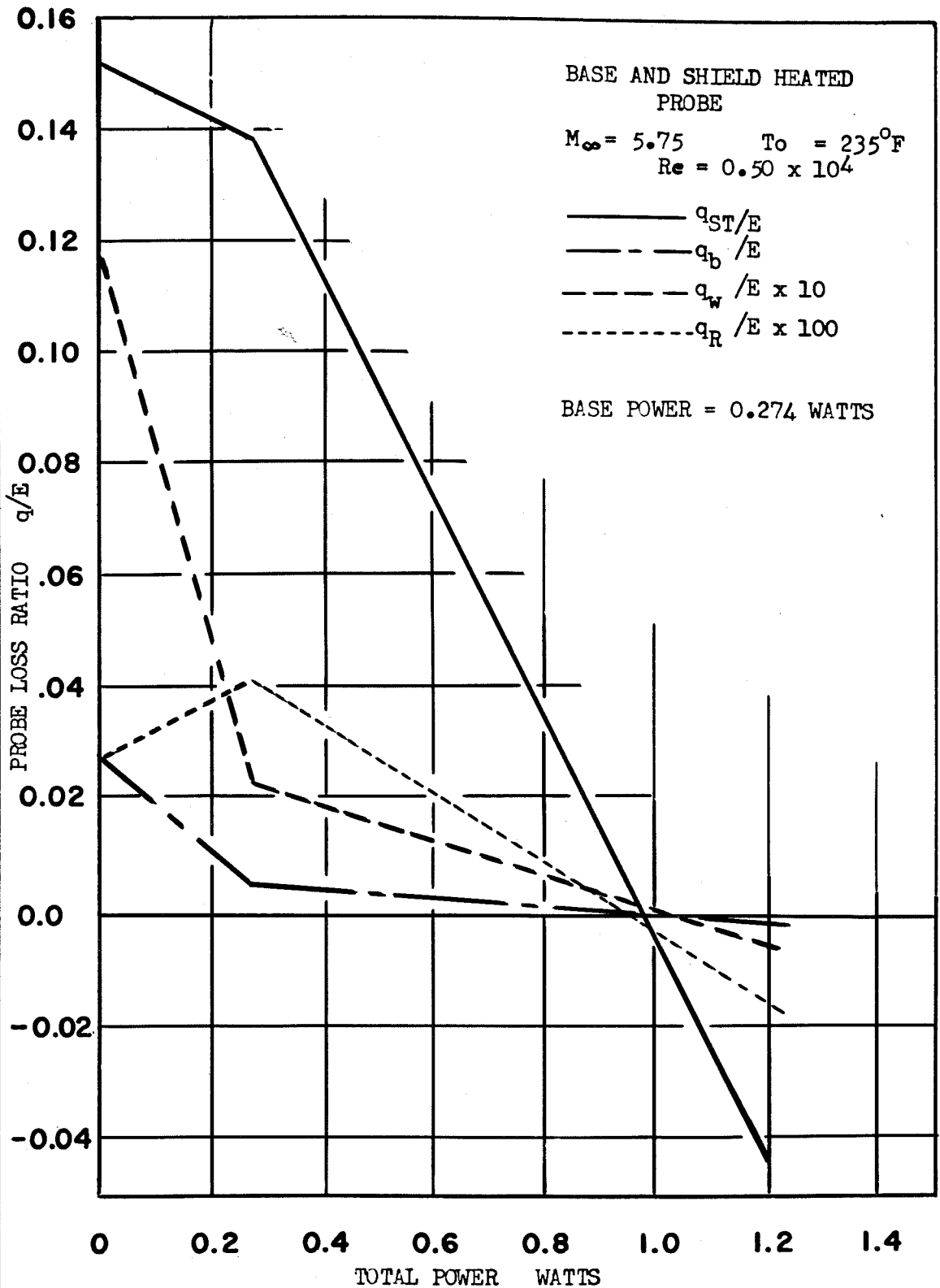


FIGURE 18 PROBE LOSS RATIO VERSUS TOTAL POWER SUPPLIED FOR
BASE AND SHIELD HEATED PROBE $P_b = 0.274$ WATTS

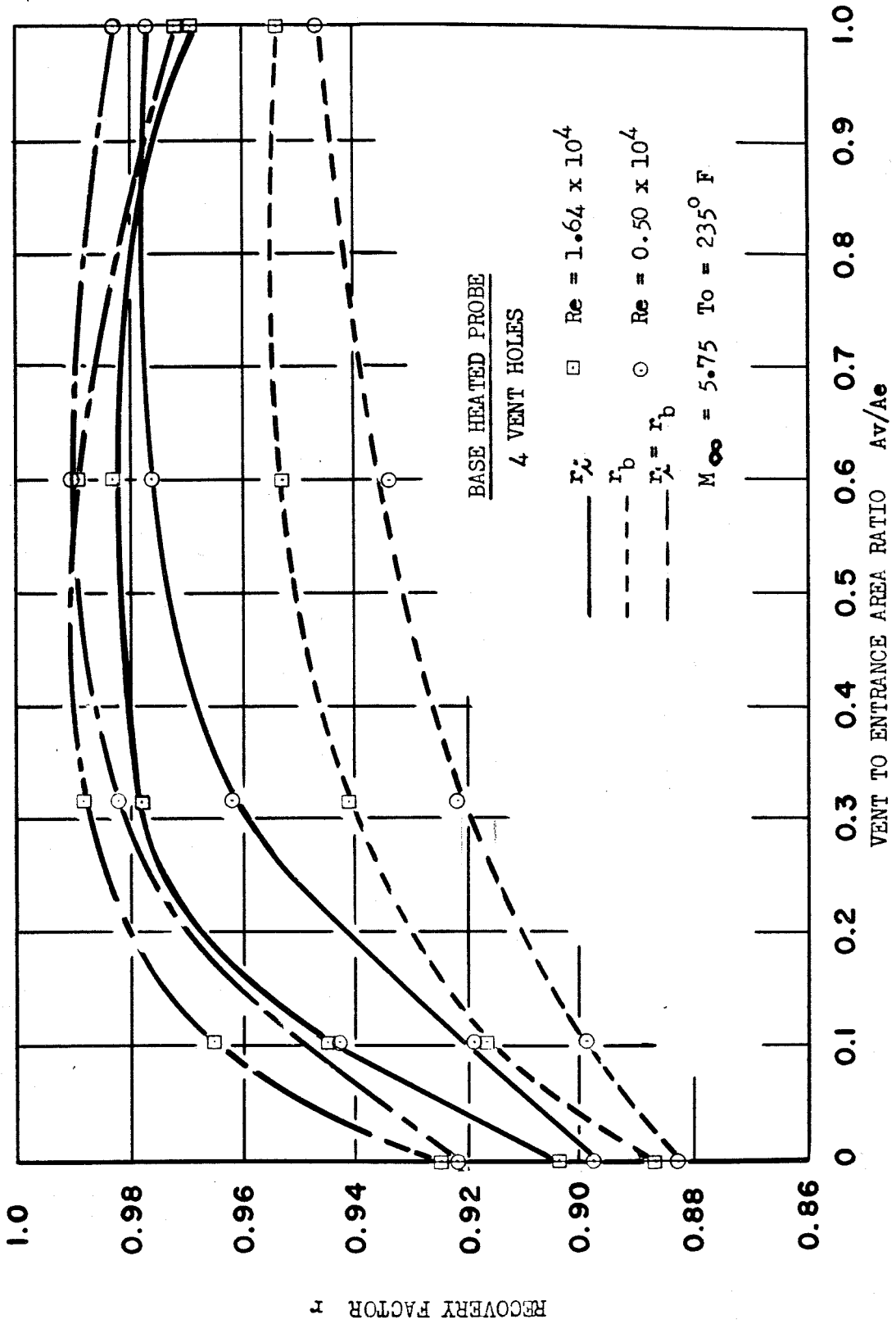
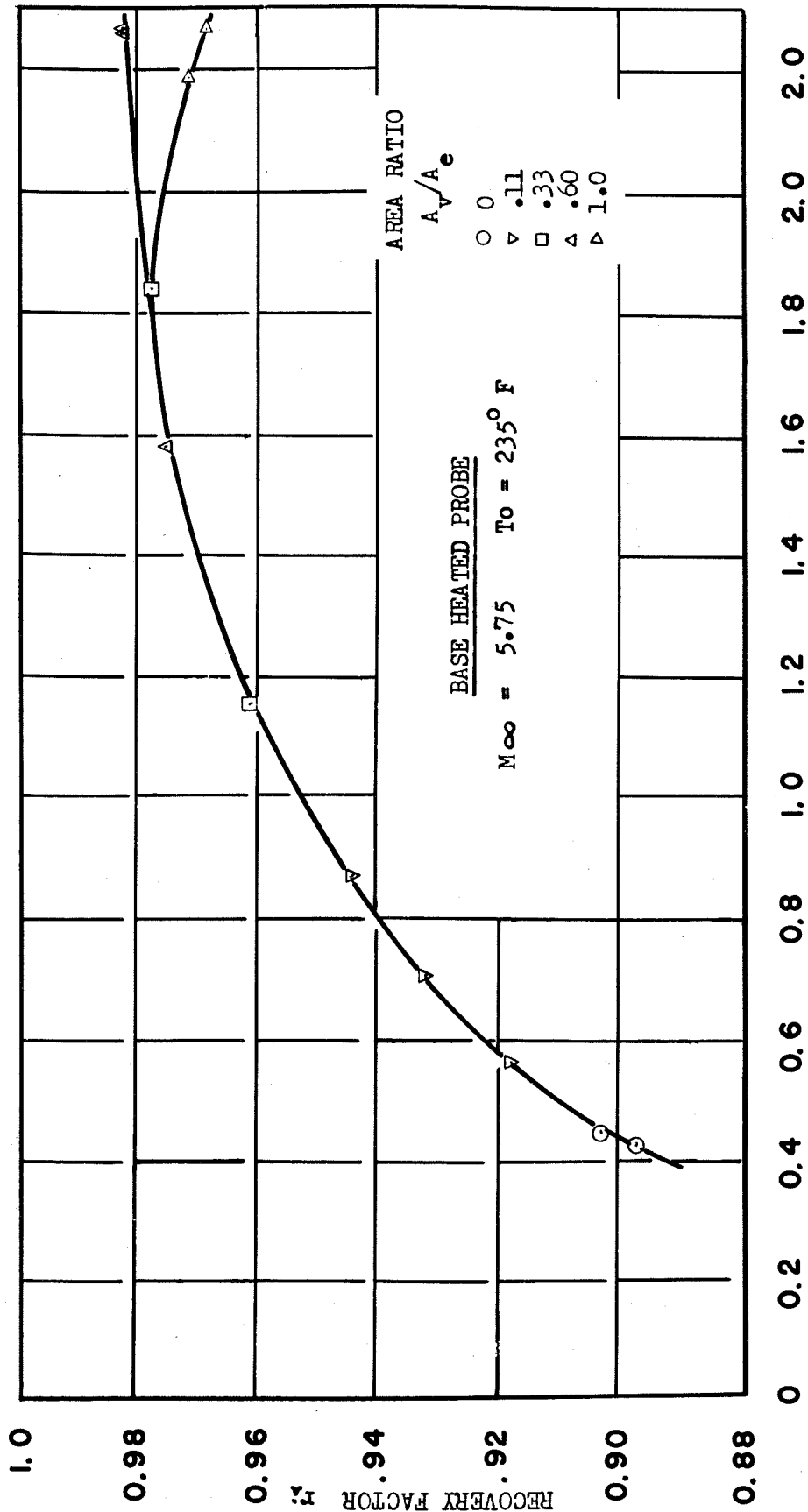
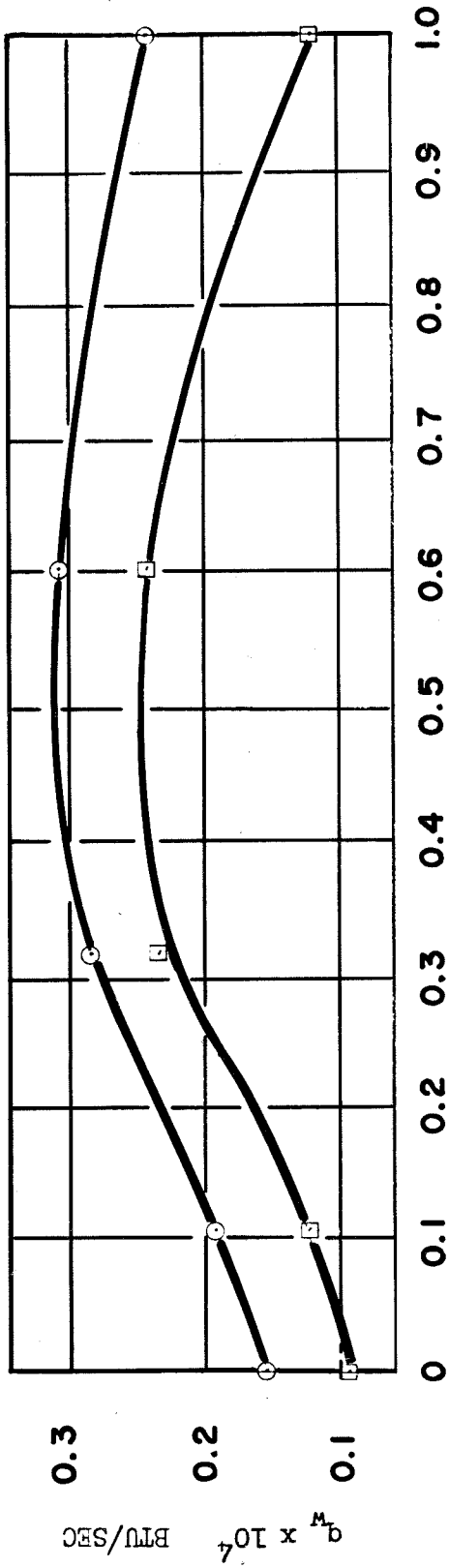


FIGURE 19 RECOVERY FACTOR VERSUS VENT TO ENTRANCE AREA RATIO AT $M_\infty = 5.75$



CONVECTIVE HEAT TRANSFER COEFFICIENT $h_w \times 10^4$ BTU/SEC - in² - °R

FIGURE 20 RECOVERY FACTOR VERSUS THERMOCOUPLE CONVECTIVE HEAT TRANSFER COEFFICIENT FOR SEVERAL VENT TO ENTRANCE AREA RATIOS AT $M_{\infty} = 5.75$



$M_\infty = 5.75$
 $T_o = 235^\circ \text{F}$
BASE HEATED PROBE
 \circ $Re = 0.50 \times 10^4$
 \square $Re = 1.64 \times 10^4$

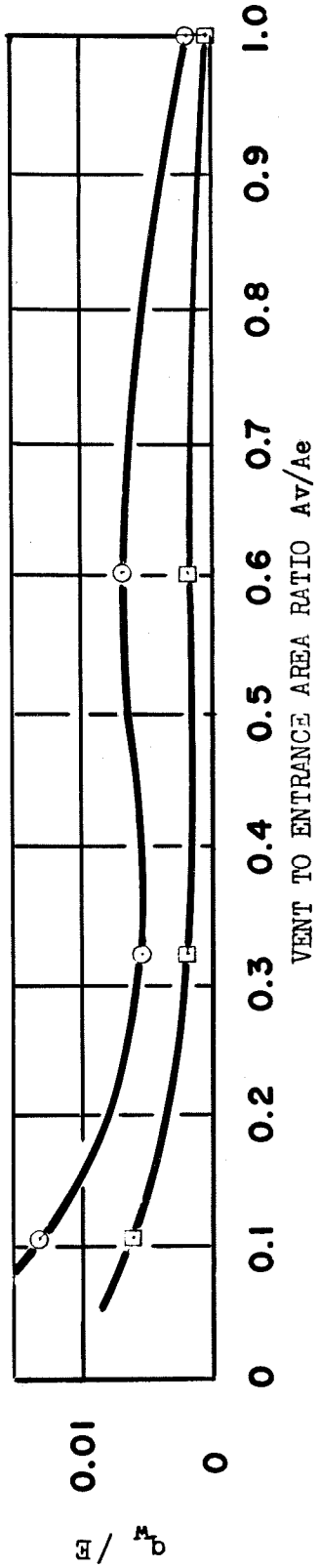


FIGURE 21 THERMOCOUPLE CONDUCTION HEAT TRANSFER VERSUS VENT TO ENTRANCE AREA RATIO AT $M_\infty = 5.75$

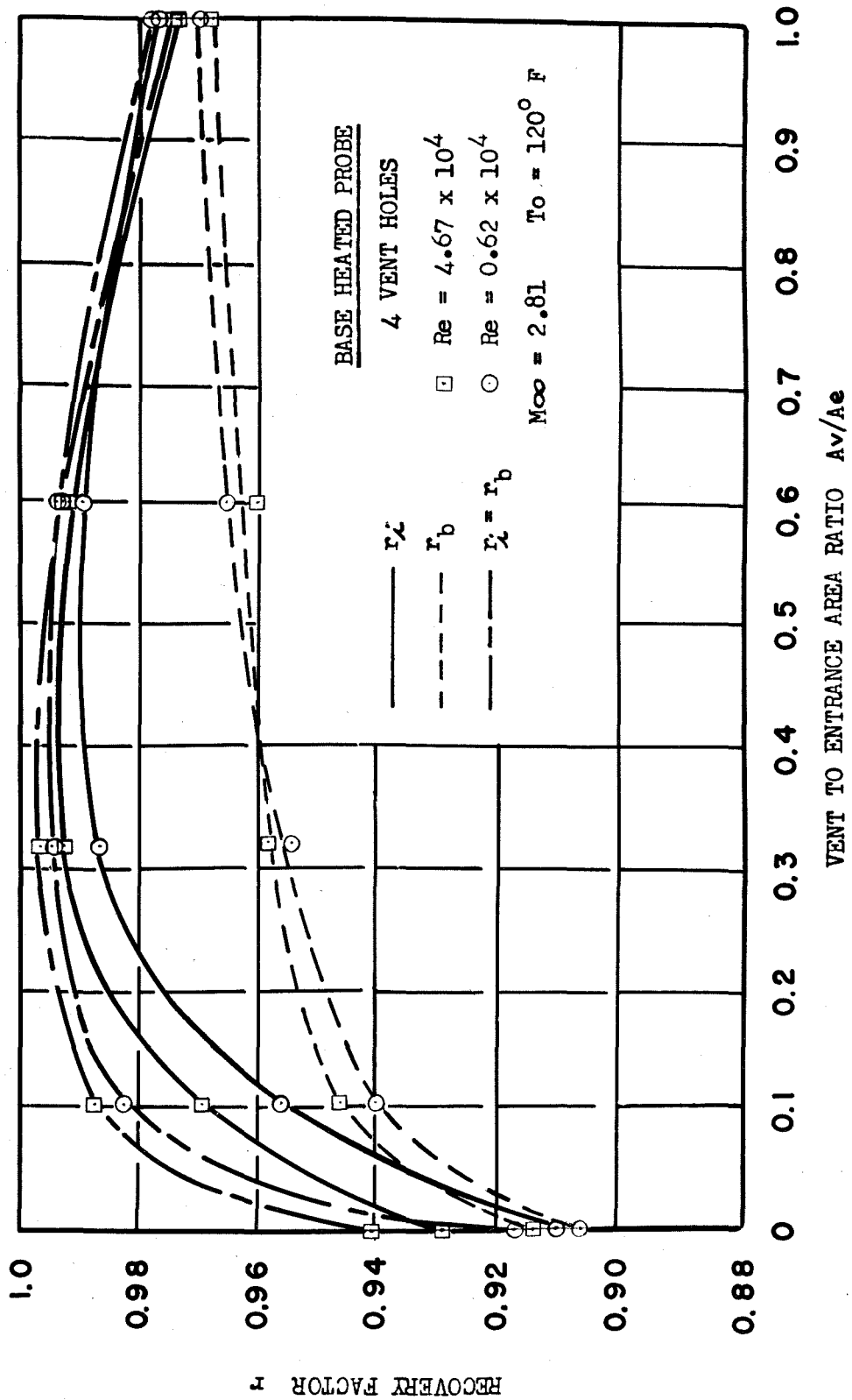


FIGURE 22 RECOVERY FACTOR VERSUS VENT TO ENTRANCE AREA RATIO AT $M_\infty = 2.81$

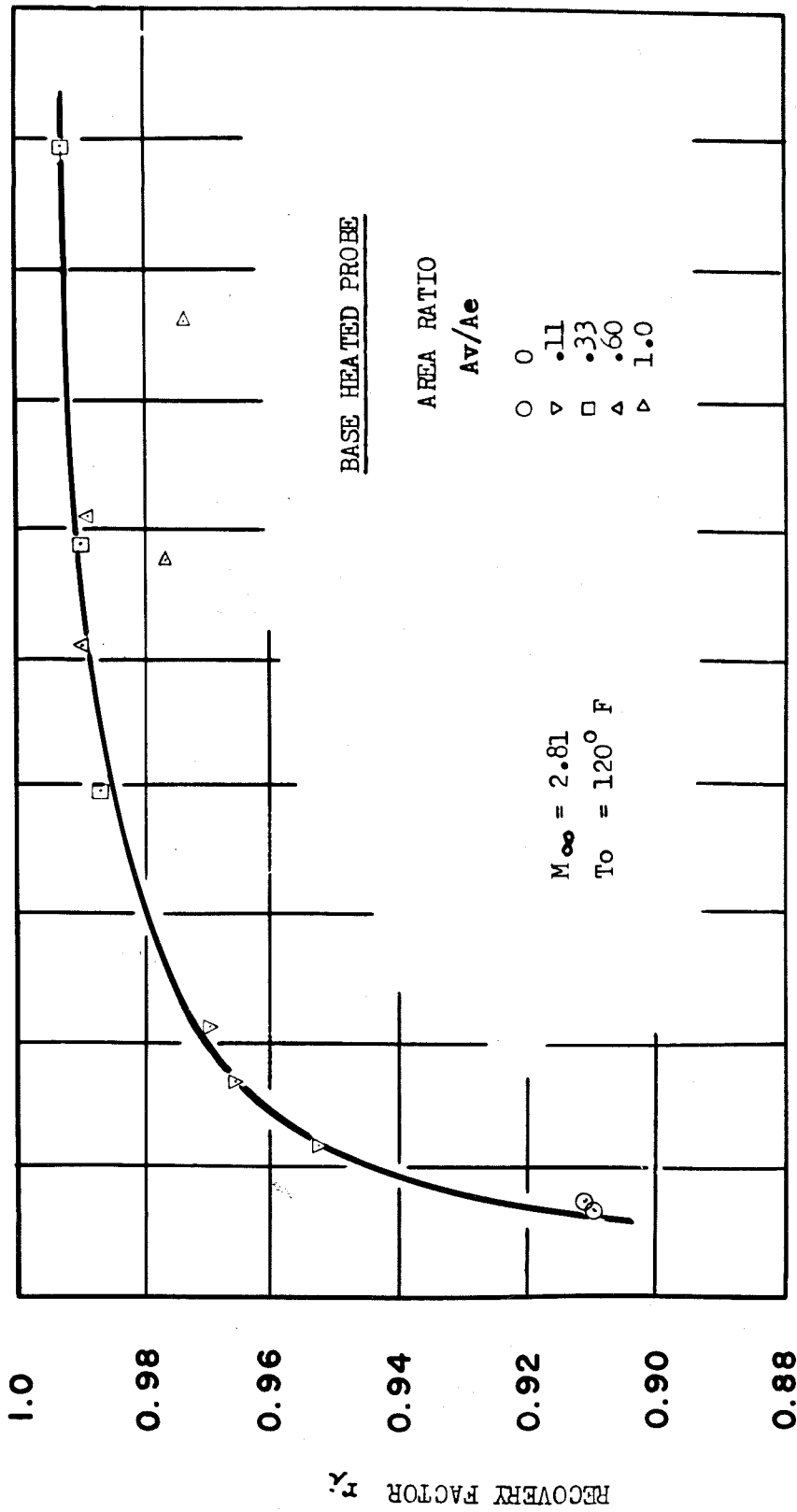
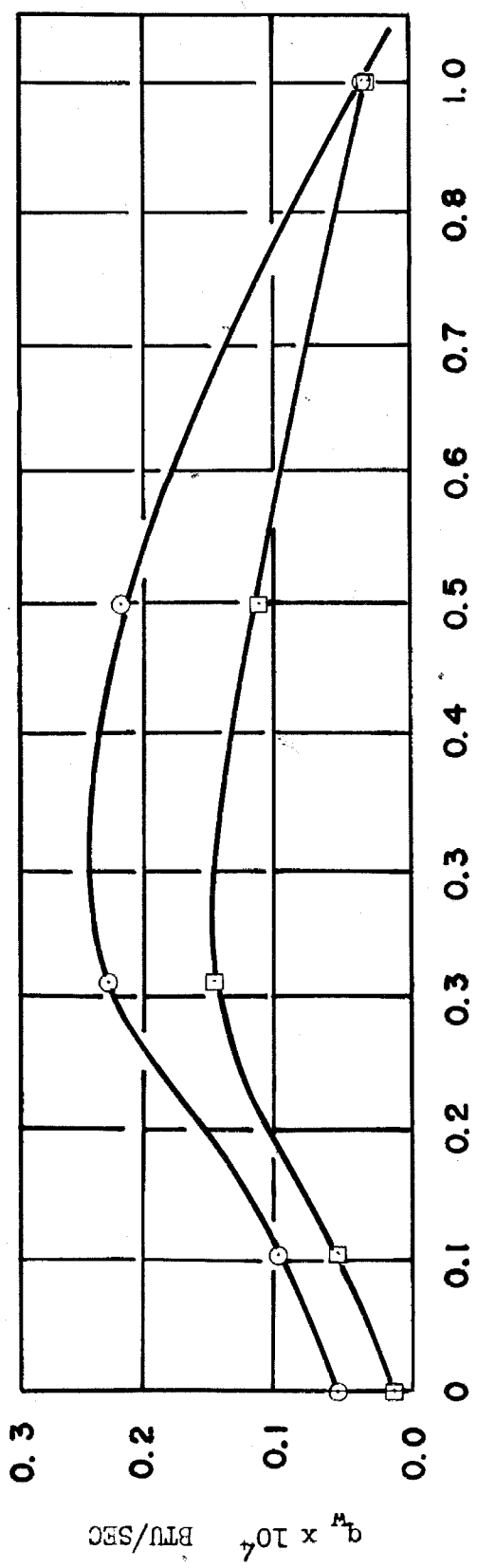


FIGURE 23 RECOVERY FACTOR VERSUS THERMOCOUPLE CONVECTIVE HEAT TRANSFER COEFFICIENT FOR SEVERAL VENT TO ENTRANCE AREA RATIOS AT $M_\infty = 2.81$



BASE HEATED PROBE

$M_\infty = 2.81$
 $T_0 = 120^\circ F$

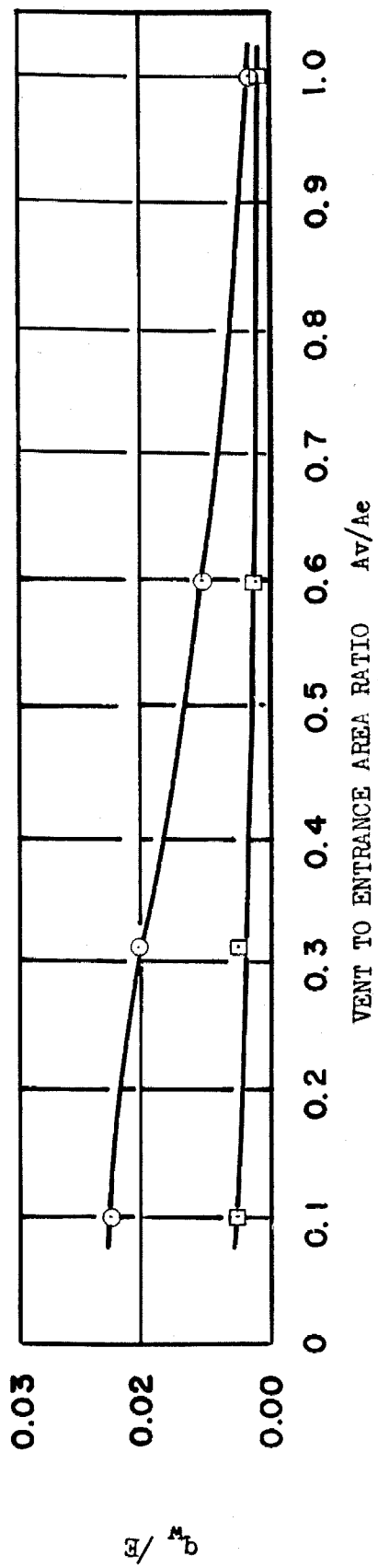


FIGURE 24. THERMOCOUPLE CONDUCTION HEAT TRANSFER VERSUS VENT TO ENTRANCE AREA RATIO AT $M_\infty = 2.81$

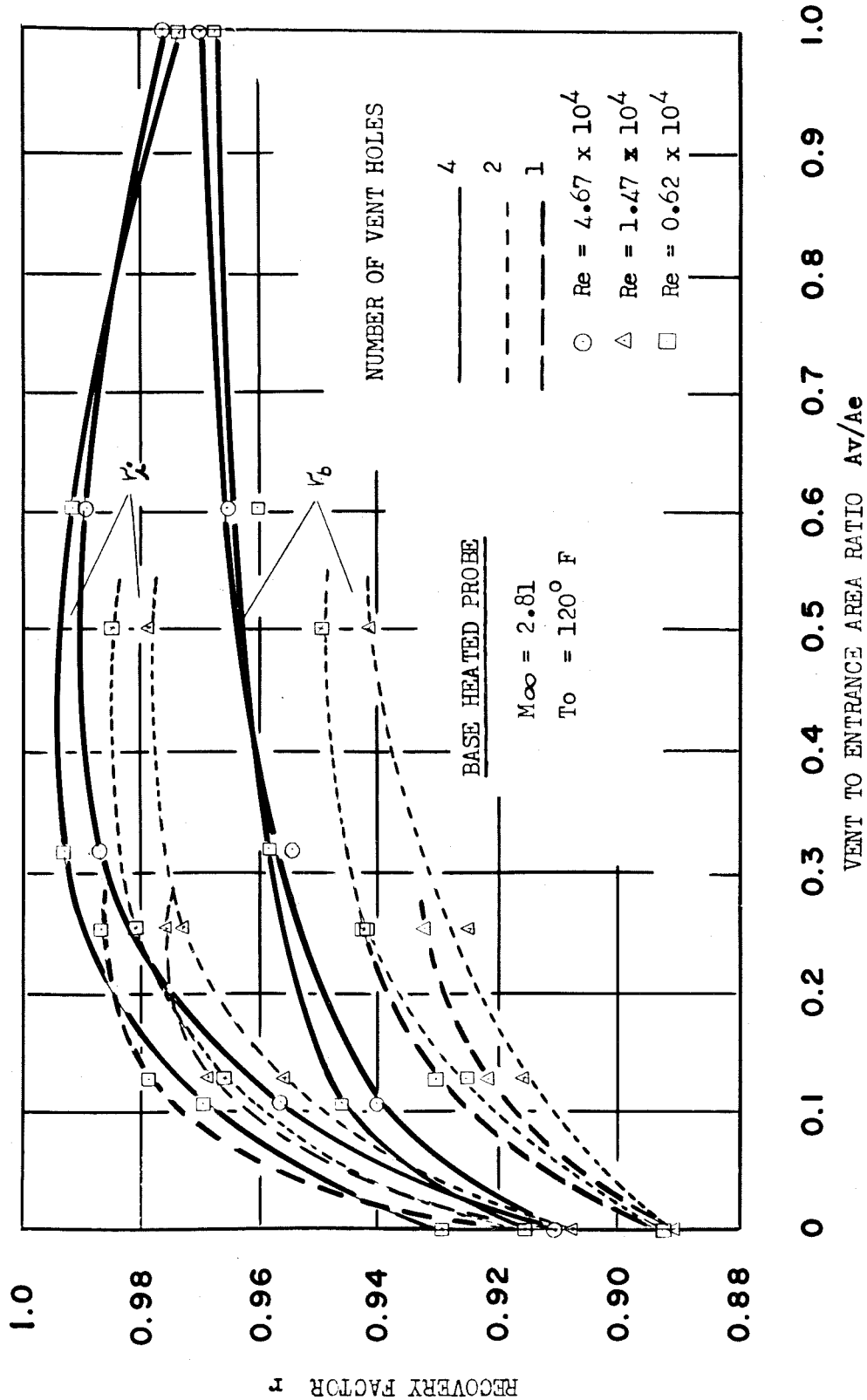


FIGURE 25 EFFECT OF NUMBER OF VENT HOLES ON RECOVERY FACTOR

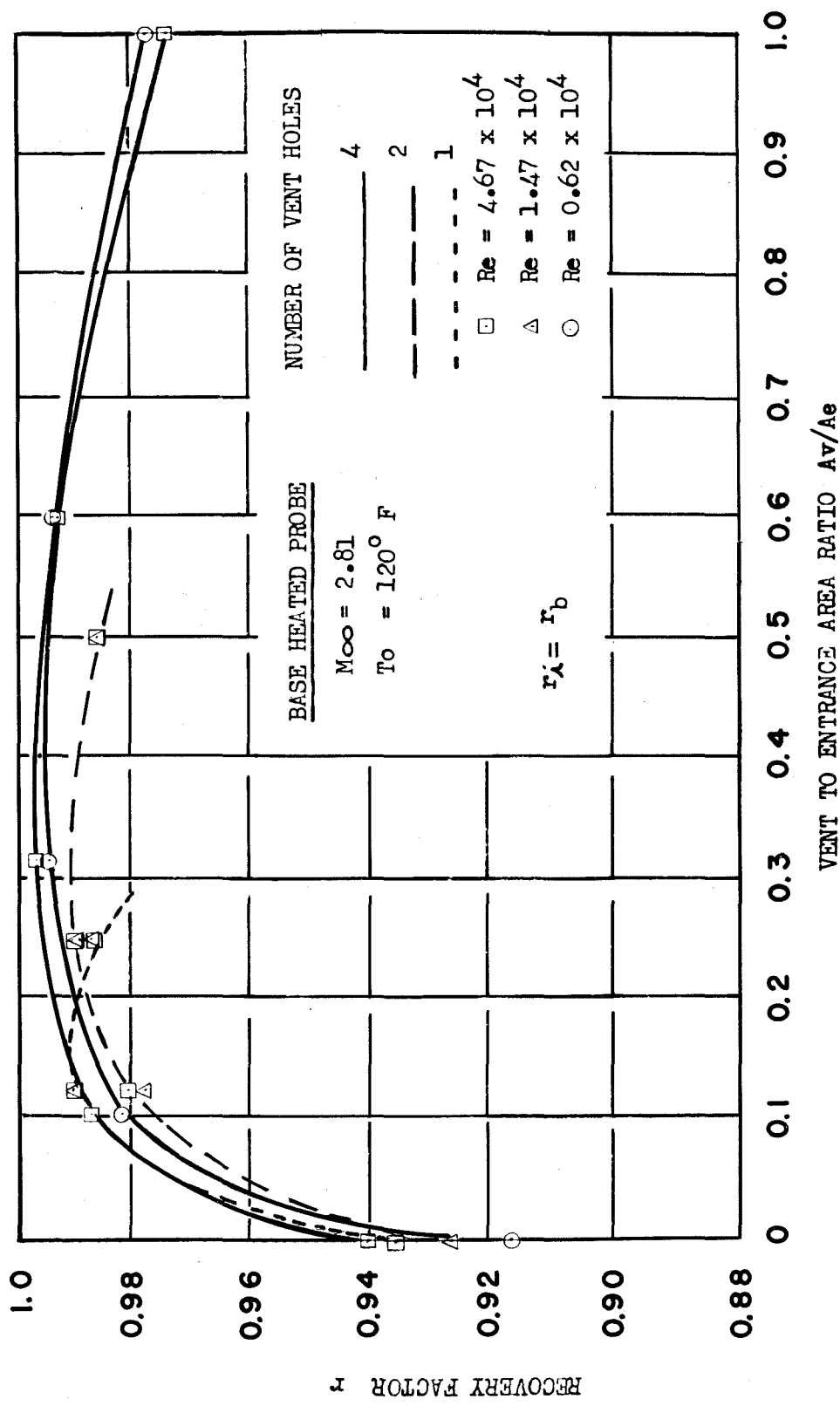
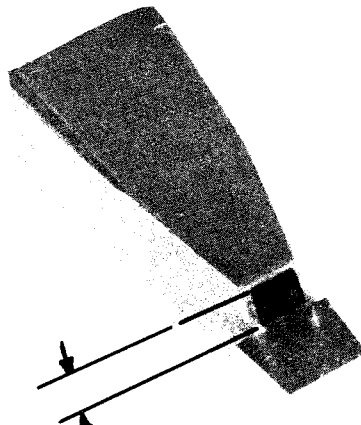
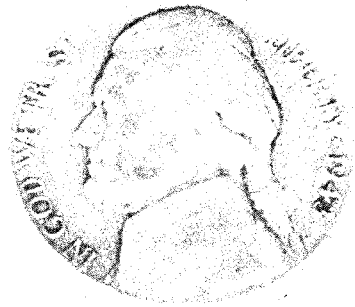


FIGURE 26 EFFECT OF HEATED BASE ON OPTIMUM VENT HOLE SIZE AND NUMBER



PLATINUM PLATED
VYCOR SHIELD
 $A_v/A_e = 1.0$
4 VENT HOLES



0.05 in I.D. SQUARE

0.01 in LIP

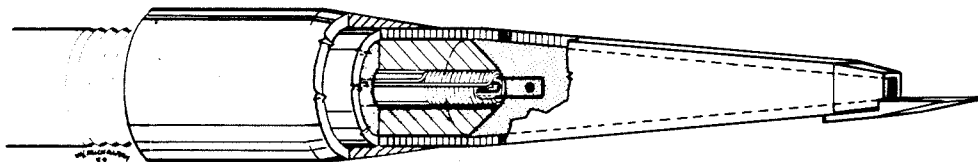
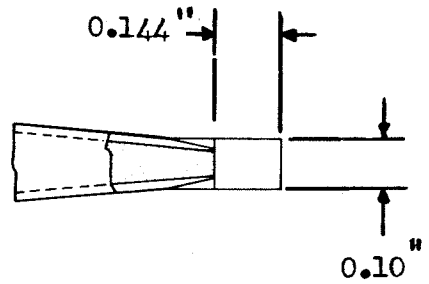


FIGURE 27 BASE HEATED RAMP PROBE

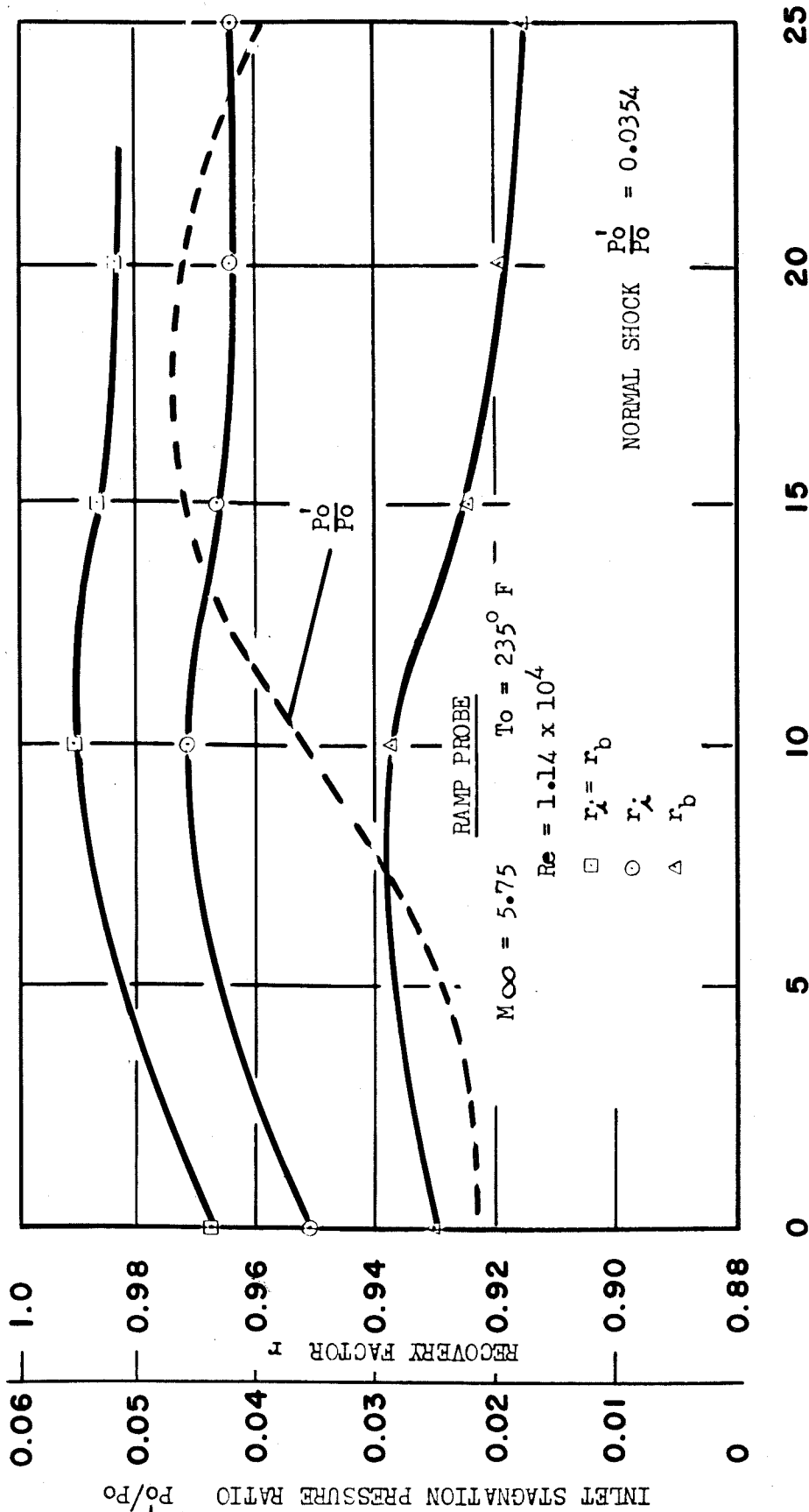


FIGURE 28 RECOVERY FACTOR VERSUS ANGLE OF ATTACK FOR RAMP PROBE

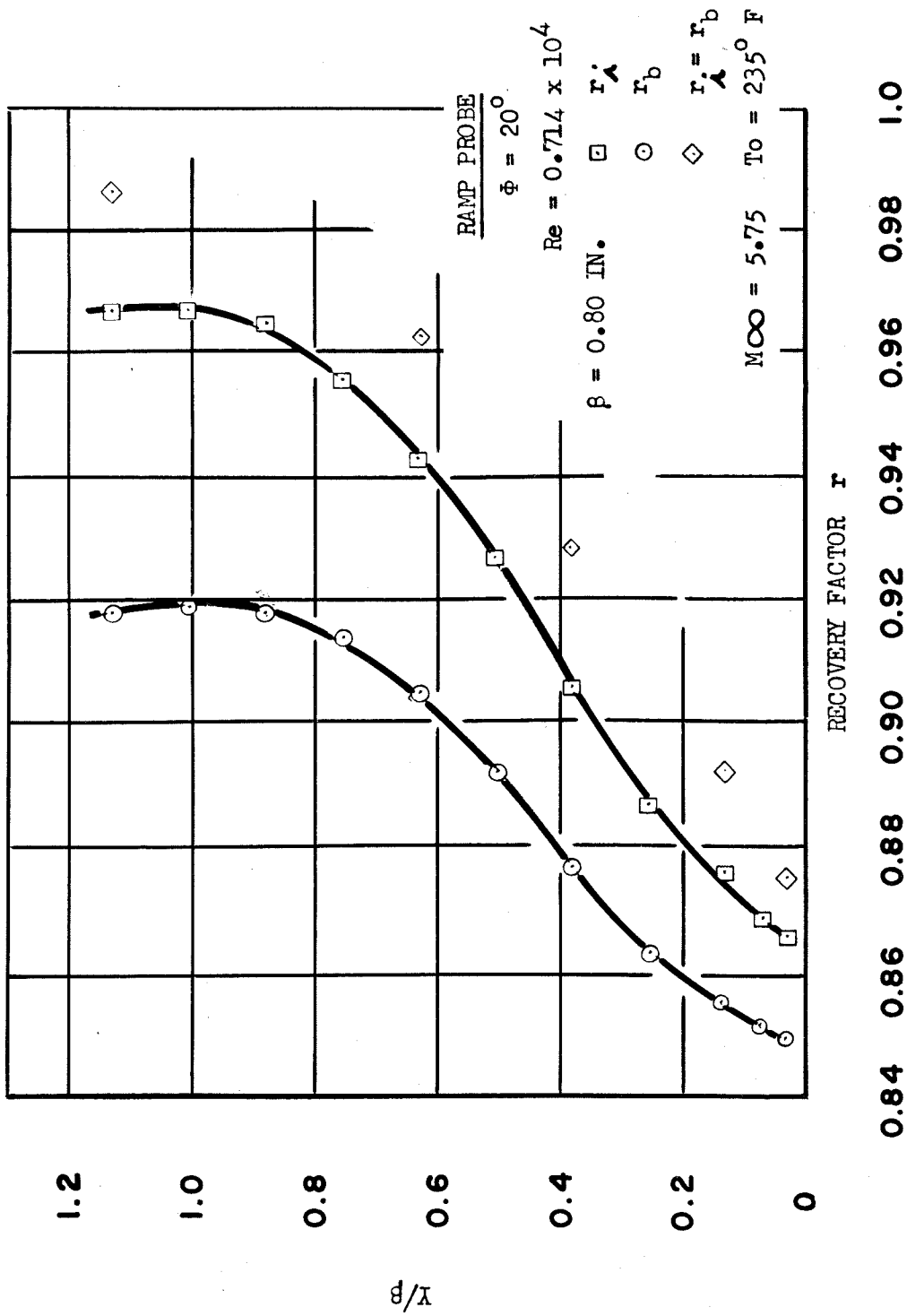


FIGURE 29 TUNNEL WALL TEMPERATURE BOUNDARY LAYER SURVEY AT $M_\infty = 5.75$

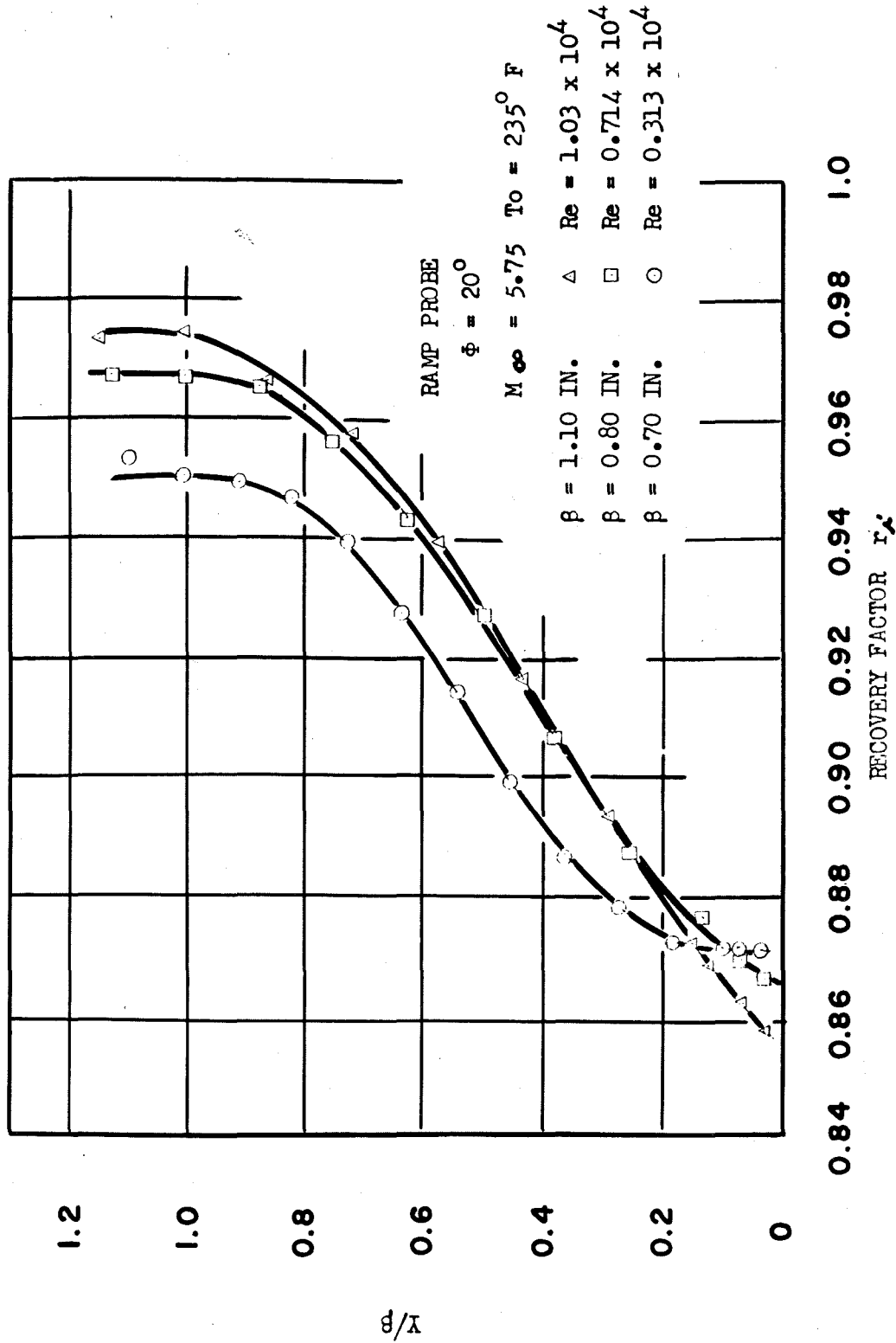
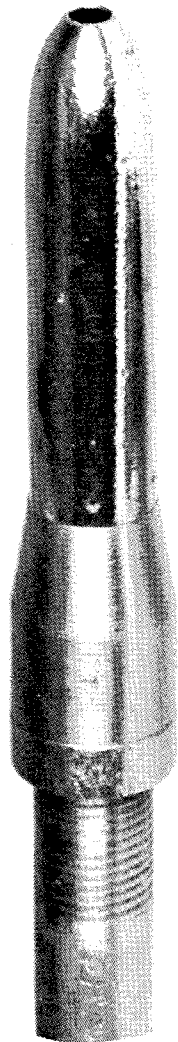
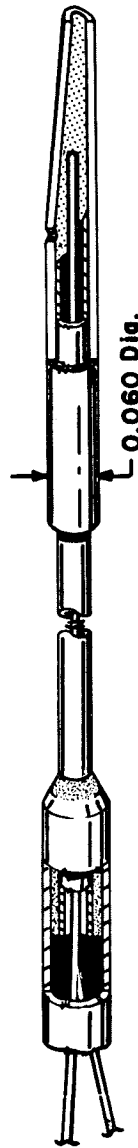


FIGURE 30 TUNNEL WALL TEMPERATURE BOUNDARY LAYER SURVEY FOR THREE REYNOLDS NUMBERS



HIGH THERMOCOUPLE LENGTH OVER DIAMETER RATIO PROBE CERAMIC SHIELD
 $(L/D) = 100$ $A_v/A_e = 0.167$
 4 VENT HOLES
 PLATINUM PLATED



0.020"

0.060 Dia.

BOUNDARY LAYER PROBE (#5)
 $L/D = 15$ $A_v/A_e = 1.3$
 1 VENT HOLE
 VYCOR SHIELD
 GOLD PLATED

FIGURE 31 BOUNDARY LAYER AND HIGH (L/D) PROBE

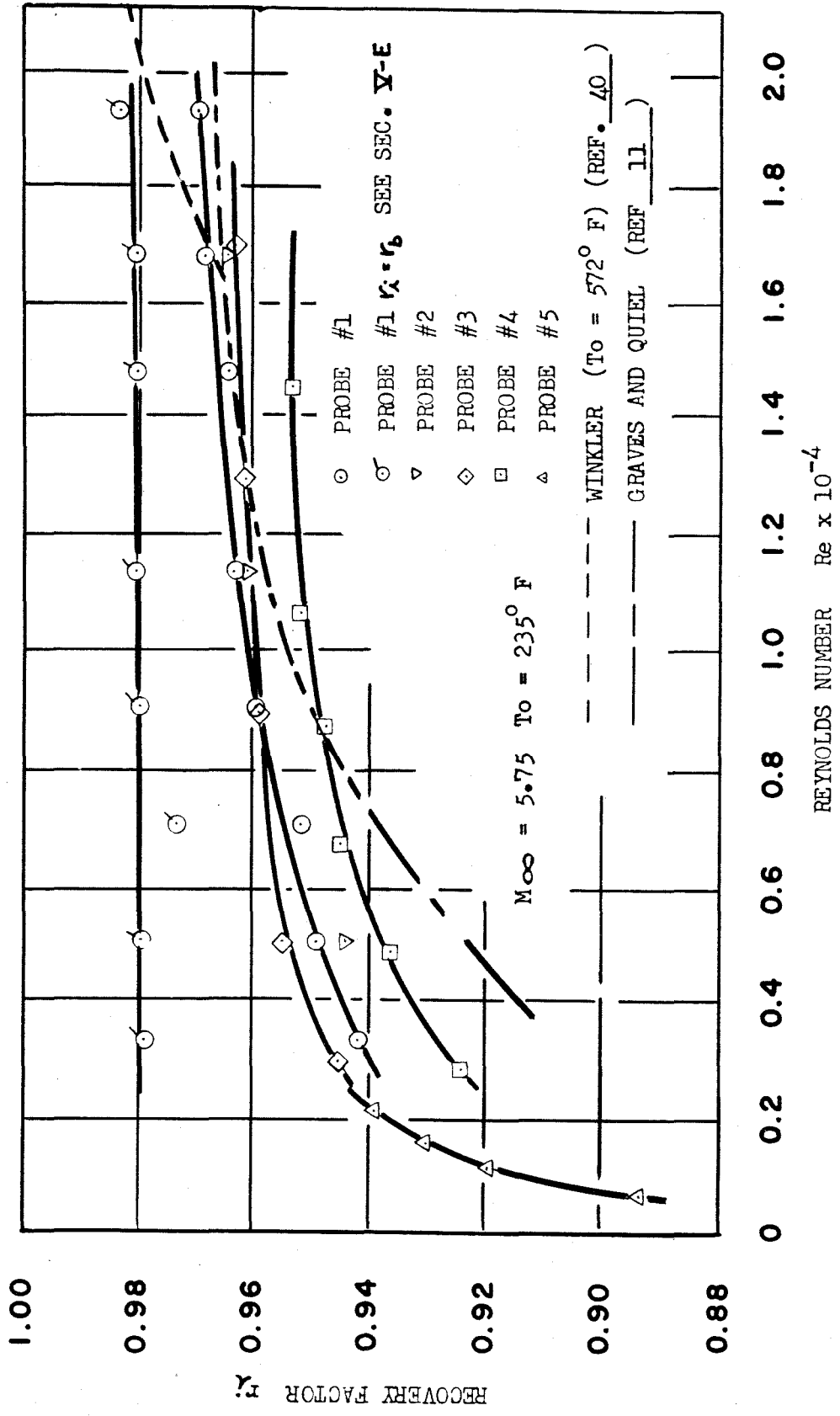


FIGURE 32 RECOVERY FACTORS FOR SEVERAL TYPICAL PROBES